1-1-2019

Optimal Design and Planning of Hybrid AC/DC Microgrid

Hossein Lotfi
University of Denver

Optimal Design and Planning of Hybrid AC/DC Microgrid

Abstract

The traditional approach for microgrid design and deployment has been mainly focused on AC systems. DC microgrids, however, are gaining attention due to numerous advantages they provide over AC microgrids, such as removing the need for synchronization and frequency adjustment as well as appropriateness in supporting DC loads and distributed energy resources (DERs). Moreover, considering that both AC and DC DERs are utilized in microgrids, hybrid microgrids would provide viable and economic solutions as they can potentially eliminate the need for AC-to-DC or DC-to-AC voltage conversions. This dissertation focuses on a hybrid microgrid planning model with the objective of minimizing the microgrid total planning cost. The model determines the optimal DER size and generation mix, the point of connection of DERs, and the type of each feeder, i.e., AC or DC. Moreover, it identifies threshold ratios of AC/DC loads at each feeder causing one type of feeder to be more economical than the other. It also proposes a co-optimization generation and distribution planning model in microgrids in which simultaneous investment in generation, i.e., distributed generation (DG) and distributed energy storage (DES), and distribution, i.e., upgrading the existing distribution network, is considered. Since uncertainty considerations in microgrid operation and planning are of high importance and uncertain factors can potentially alter the microgrid planner's decisions, this dissertation investigates a detailed discussion and analysis of prevailing uncertainties in microgrid operation and planning. New mathematical approaches, such as robust optimization, are commonly adopted to capture uncertainties and ensure practicality. However, this added practicality is at the expense of increased problem size and computational complexity. This dissertation accordingly proposes a new preprocessing approach to integrate uncertainties while reducing computational requirements.

Numerical simulations exhibit the merits of the proposed microgrid planning and co-optimization generation and distribution planning models in microgrid by analyzing the sensitivity of solutions on various decisive planning factors and reveal the effectiveness of the proposed preprocessing approach over the commonly used robust optimization method from the execution time and practicality perspectives.

Document Type

Dissertation

Degree Name

Ph.D.

Department

Electrical Engineering

First Advisor

Amin Khodaei, Ph.D.

Second Advisor

Andrew Goetz, Ph.D.

Third Advisor

David Gao, Ph.D.

OPTIMAL DESIGN AND PLANNING OF HYBRID AC/DC MICROGRID

_____

A Dissertation

Presented to

the Faculty of the Daniel Felix Ritchie School of Engineering and Computer Science

University of Denver

_____

In Partial Fulfillment

of the Requirements for the Degree

Doctor of Philosophy

_____

by

Hossein Lotfi

June 2019

Advisor: Dr. Amin Khodaei

Author: Hossein Lotfi
Title: OPTIMAL DESIGN AND PLANNING OF HYBRID AC/DC MICROGRID
Advisor: Dr. Amin Khodaei
Degree Date: June 2019

Abstract

The traditional approach for microgrid design and deployment has been mainly focused on AC systems. DC microgrids, however, are gaining attention due to numerous advantages they provide over AC microgrids, such as removing the need for synchronization and frequency adjustment as well as appropriateness in supporting DC loads and distributed energy resources (DERs). Moreover, considering that both AC and DC DERs are utilized in microgrids, hybrid microgrids would provide viable and economic solutions as they can potentially eliminate the need for AC-to-DC or DC-to-AC voltage conversions. This dissertation focuses on a hybrid microgrid planning model with the objective of minimizing the microgrid total planning cost. The model determines the optimal DER size and generation mix, the point of connection of DERs, and the type of each feeder, i.e., AC or DC. Moreover, it identifies threshold ratios of AC/DC loads at each feeder causing one type of feeder to be more economical than the other. It also proposes a co-optimization generation and distribution planning model in microgrids in which simultaneous investment in generation, i.e., distributed generation (DG) and distributed energy storage (DES), and distribution, i.e., upgrading the existing distribution network, is considered. Since uncertainty considerations in microgrid operation and planning are of high importance and uncertain factors can potentially alter the microgrid planner's decisions, this dissertation investigates a detailed discussion and analysis of prevailing uncertainties in microgrid operation and planning. New mathematical approaches, such as

robust optimization, are commonly adopted to capture uncertainties and ensure practicality. However, this added practicality is at the expense of increased problem size and computational complexity. This dissertation accordingly proposes a new preprocessing approach to integrate uncertainties while reducing computational requirements.

Numerical simulations exhibit the merits of the proposed microgrid planning and co-optimization generation and distribution planning models in microgrid by analyzing the sensitivity of solutions on various decisive planning factors and reveal the effectiveness of the proposed preprocessing approach over the commonly used robust optimization method from the execution time and practicality perspectives.

Acknowledgement

There are many people that have earned my gratitude for their contribution to my time in my PhD program. More specifically, I would like to thank my advisor, my dissertation committee members, my friends, and my family.

First, I would like to express my sincere gratitude to my advisor and Chair of the Department of Electrical and Computer Engineering at University of Denver, Dr. Amin Khodaei. Since my first day in graduate school, Dr. Khodaei believed in me like nobody else and gave me endless support, guidance, and encouragement throughout my education. I am truly grateful for all his support and consideration.

Furthermore, I would like to enthusiastically thank my committee members, Dr. Andrew Goetz, Dr. David Gao, and Dr. Mohammad Matin, for their time, great support, and invaluable advice. I also show gratitude for JB Holston, Dean of Ritchie School of Engineering and Computer Science, for his supports. Besides, I would like to thank my lab mates at University of Denver and all my friends in Denver for all their continued support.

I profoundly thank my lovely parents, grandparents, and brothers for their unlimited support and persuasion. I would like to express my deepest gratitude to them for all their sacrifices, encouragements, and best wishes throughout my life.

My special thanks go to my sympathetic, lovely, and fabulous wife, Maryam. In the toughest times, she has been my best advocate. Words cannot express how thankful I am to her for all her love, supports, and patience in the past years.

Table of Contents

1. Chapter One: Introduction 1
    - 1.1 Importance of Microgrids 1
    - 1.2 AC/DC Microgrids 2
    - 1.3 AC Versus DC Microgrid Planning 3
    - 1.4 Hybrid AC/DC Microgrid Planning 6
    - 1.5 Co-Optimization Generation and Distribution Planning in Microgrids 9

2. Chapter Two: AC Versus DC Microgrid Planning 12
    - 2.1 Model Outline 13
    - 2.2 Problem Formulation 15
    - 2.3 Numerical Simulations 21
    - 2.4 Discussions 31

3. Chapter Three: Hybrid AC/DC Microgrid Planning 33
    - 3.1 Model Outline 33
    - 3.2 Problem Formulation 35
    - 3.3 Numerical Simulations 39
    - 3.4 Discussions 49

4. Chapter Four: Co-Optimization Generation and Distribution Planning in Microgrids 51
    - 4.1 Model Outline and Formulation of Co-Optimization Generation and Distribution Planning in Microgrids 53
    - 4.2 Model Outline and Formulation of Microgrid Optimal Scheduling Under Uncertainties 58
        - 4.2.1 Uncertainty Control 61
    - 4.3 Proposed Preprocessing Approach 62
    - 4.4 Numerical Simulations 65
        - 4.4.1 Co-Optimization Generation and Distribution Planning 65
        - 4.4.2 Preprocessing Approach to Identify Uncertainties 72

5. Chapter Five: Conclusion and Future Directions 77

References 80

List of Figures

Chapter Two
Fig. 2.1 General structure of DC microgrids 14
Fig. 2.2 General structure of AC microgrids 15
Fig. 2.3 Annual average value of load and solar generation (MW), and the market price ($/MWh) for 24 hours 25

Chapter Three
Fig. 3.1 General structure of a hybrid AC/DC microgrid 34

Chapter Four
Fig. 4.1 IEEE 33-bus test system. 66
Fig. 4.2 Impact of the proposed signal for load uncertainties. 74
Fig. 4.3 Impact of the proposed signal for renewable uncertainties. 74
Fig. 4.4 Impact of the proposed signal for market price uncertainties. 75

List of Tables

Chapter Two

Table 2.1 Dispatchable Units Characteristics 22
Table 2.2 Nondispatchable Units Characteristics 22
Table 2.3 DES Characteristics 22
Table 2.4 Annualized Investment Cost of Converters 22
Table 2.5 Installed DER Capacity (MW) with Respect to Ratio of DC Loads 25
Table 2.6 Microgrid Costs with Respect to Ratio of DC Loads 25
Table 2.7 Installed DER Capacity (MW) with Respect to Ratio of Critical Loads 27
Table 2.8 Microgrid Costs with Respect to Ratio of Critical Loads..... 27
Table 2.9 Microgrid Costs with Respect to Converters' Efficiency..... 28
Table 2.10 Installed DER Capacity (MW) with Respect to Market Prices 29
Table 2.11 Microgrid Costs with Respect to Market Prices 29

Chapter Three

Table 3.1 Dispatchable Units Cost Coefficients of Different Steps 40
Table 3.2 Feeder Types and Installed DER Capacity (MW) with Respect to Ratio of DC Loads..... 42
Table 3.3 Microgrid Costs with Respect To Ratio Of DC Loads..... 43
Table 3.4 Feeder Types and Installed DER Capacity (MW) with Respect to Ratio of Critical Loads 45
Table 3.5 Microgrid Costs with Respect to Ratio Of Critical Loads..... 45
Table 3.6 Feeder Types and Installed DER Capacity (MW) with Respect to Converters' Efficiency..... 46
Table 3.7 Microgrid Costs with Respect to Converters' Efficiency..... 47
Table 3.8 Installed DER Capacity (MW) with Respect to Market Prices 47
Table 3.9 Microgrid Costs with Respect to Market Prices 48

Chapter Four

Table 4.1 Candidate DGs Characteristics 66
Table 4.2 Candidate DES Characteristics..... 66
Table 4.3 Candidate Lines Characteristics..... 67
Table 4.4 Investment Plan with Respect to Changes in Ratio of Critical Loads.. 68
Table 4.5 Microgrid Costs with Respect to Ratio of Critical Loads..... 68
Table 4.6 Investment Plan with Respect to Load Changes..... 69
Table 4.7 Microgrid Costs with Respect to Load Changes 70
Table 4.8 Investment Plan with Respect to Market Price Changes 71
Table 4.9 Microgrid Costs with Respect to Market Price Changes..... 72
Table 4.10 Comparison Between the Robust Optimization Problem and the Proposed Preprocessing Approach 76

Nomenclature

Abbreviations

AC	Alternating Current
CHP	Combines Heat and Power
DC	Direct Current
DER	Distributed Energy Resource
DES	Distributed Energy Storage
DG	Distributed Generation
DSO	Distribution System Operator
HVDC	High Voltage DC
MILP	Mixed Integer Linear Programming
POI	Point of Interconnection
VOLL	Value of Lost Load

Indices

b	Index for hour
ch	Superscript for DES charging mode
dch	Superscript for DES discharging mode
g	Superscript for uncertain renewable generation
h	Index for day
i	Index for DERs
inv	Subscript for DC-to-AC inverters
k	Index for feeders
l	Index for lines
m, n	Index for buses
q	Index for various steps of the cost coefficient of dispatchable DGs
rec	Subscript for AC-to-DC rectifiers
s	Index for scenarios
t	Index for year

^	Index for calculated/given variables
~	Index for forecasted parameters

Sets

B	Set of buses
B_l	Set of buses at both ends of line *l*
D	Set of dual variables
G	Set of all dispatchable units
G_{ac}	Set of AC dispatchable units
G_{dc}	Set of DC dispatchable units
I	Set of DC-to-AC inverters
L	Set of lines
L_m	Set of lines connected to bus *m*
P	Set of primal variables
R	Set of AC-to-DC rectifiers
S	Set of DESs
U	Set of uncertain parameters
W	Set of all nondispatchable units
W_{ac}	Set of AC nondispatchable units
W_{dc}	Set of DC nondispatchable units

Parameters

a_1/a_2	Line-bus connection indicator (1 if connected at from/to bus, 0 otherwise)
b	Line susceptance
c	Generation price for dispatchable units
CC	Annualized DG investment cost
CE	Annualized DES investment cost – energy
CI	Annualized investment cost of DC-to-AC inverters
CL	Annualized line investment cost

CP Annualized DES investment cost – power

CR Annualized investment cost of AC-to-DC rectifiers

C^{cap} Allowable DES installation capacity

g Line conductance

M Large positive constant

P^{cap} Allowable DER installation capacity

P_M^{max} Flow limit between the microgrid and utility grid

PD Active load

PD^{max} Maximum demand during the planning horizon

$PL^{\max}$ Active line flow limit

pr Probability of each scenario

QD Reactive load

$QL^{\max}$ Reactive line flow limit

r Discount rate

u_M Binary islanding parameter (1 if grid-connected, 0 if islanded)

v Value of lost load (VOLL)

Γ Budget on uncertainty option

α Ratio of DC loads

α' Ratio of AC loads

β Ratio of critical loads

η Efficiency (DES, inverters, and rectifiers)

κ Coefficient of present-worth value

ρ Market price

ζ Normalized generation forecast of nondispatchable DGs

Variables

C^{max} Installed DES capacity

IC Microgrid investment cost

LS Load curtailment

o	Line investment state (1 if installed, 0 otherwise)
OC	Microgrid operation cost
P	DER active power output
P_F	Exchange power with the utility grid at each feeder
P^M	Microgrid exchange power with the utility grid
P^{max}	Installed DER capacity
PL	Active line flow
Q	DER reactive power output
QL	Reactive line flow
RC	Microgrid reliability cost
u	Auxiliary binary variables for uncertain parameters
V	Bus voltage magnitude
w	Binary dc bus variable (1 if a dc bus is considered in the microgrid, 0 otherwise)
x	DER investment state (1 if installed, 0 otherwise)
y	Uncertain variable
z	Microgrid/Feeder investment state (0 if AC, 1 if DC)
θ	Bus voltage angle
$\lambda, \pi, \vartheta, \mu, \psi, \xi, \sigma$	Dual variables

1. Chapter One: Introduction

1.1 Importance of Microgrids

Microgrid deployments are trusted to improve power quality, reduce emissions, reduce network congestion and power losses, increase energy efficiency, and potentially improve system economics. Microgrids could also eliminate investments on additional generation and transmission facilities to supply remote loads. Moreover, microgrids islanding capability in the event of faults or disturbances in upstream networks would enhance grid and customers' reliability and resilience [1][2][3][4][5][6][7][8] [9]. During the past decade, a significant amount of research has been devoted to study microgrids and to facilitate development and implementation efforts. Microgrid deployments have been extensively supported by the federal government in the United States, particularly by establishing the U.S. DOE Microgrid Initiative [10]. There has been a considerable increase in the number of microgrid projects such that the total global installed microgrid capacity has risen from 4,393 MW in 2014 to 12,031 MW in 2015 [11], and to 16,552.8 MW in 2016 with 1,681 operating and under development projects [12]. As of the second quarter of 2017 [13], Navigant Research has identified 1,842 microgrid project entries, including 173 new projects which represent 19,279.4 MW of capacity for projects that are operating, under development, and proposed. Moreover, as of the second quarter of 2018 [14], 2134 projects have been identified in the world, representing 24,981 MW of proposed, under development, and operational

power capacity. It includes 240 new projects from 139 countries. Based on [15], North America is the leading microgrid market in terms of total capacity. The next positions belong to Asia Pacific and the Middle East & Africa.

Solar PV and energy storage feature prominently in modern microgrid systems, particularly as rural electrification and energy access programs fuel growth in the remote segment. Moreover, according to a 2016 report [12], if the microgrid growth rate holds, the market will expand 116% in four years. Additionally, GTM Research predicts the US microgrid market opportunity to double from $836 million in 2016 to $1.66 billion in 2020. These figures clearly represent the growing interest in this new technology and picture future power grids as systems of interconnected microgrids.

This dissertation investigates microgrid planning and uncertainty consideration in microgrids while focuses on AC, DC, and hybrid microgrids.

1.2 AC/DC Microgrids

Microgrids can be categorized into different groups based on the type (such as campus, military, residential, commercial, and industrial), the size (such as small, medium, and large scales), the application (such as premium power, resilience-oriented, loss reduction, etc.), and the connectivity (remote and grid-connected). Based on the voltages and currents adopted in a microgrid, however, three microgrid types can be identified: AC, DC, and hybrid. In AC microgrids, all distributed energy resources (DERs) and loads are connected to a common AC bus. DC generating units as well as distributed energy storage (DES) will be connected to the AC bus via DC-to-AC inverters, and further, AC-to-DC rectifiers are used for supplying DC loads. In DC microgrids, however, the common bus is DC, where AC-to-DC rectifiers are used for

connecting AC generating units, and DC-to-AC inverters are used for supplying AC loads. In hybrid microgrids, which could be considered as a combination of AC and DC microgrids, both types of buses exist, where the type of connection to each bus depends on the proximity of the DER/load to the bus. Extensive studies can be found on different aspects of microgrids operation and control, where the majority of these studies focus on AC microgrids, perceivably due to the connection to the AC utility grid and the utilization of AC DERs. DC microgrids could however offer several advantages when studied in detail and compared with AC microgrids: 1) higher efficiency and reduced losses due to the reduction of multiple converters used for DC loads, 2) easier integration of various DC DERs, such as DES, solar PV, and fuel cells, to the common bus with simplified interfaces, 3) more efficient supply of DC loads, like electric vehicles and LED lights, 4) eliminating the need for synchronizing generators, which enables rotary generating units to operate at their own optimum speed, and 5) enabling bus ties to be operated without the need for synchronizing the buses [16]. These benefits, combined with the significant increase in DC loads such as personal computers, laptop computers, LED lights, data and telecommunication centers, and other applications where the typical 50-Hz and 60-Hz AC systems are not available, could potentially introduce DC microgrids as viable and economic solutions in addressing future energy needs.

1.3 AC Versus DC Microgrid Planning

The prior research on DC microgrid planning is rather limited and available studies on microgrid planning mostly focus on AC microgrids. The study in [17] proposes a planning model for AC microgrid considering uncertain physical and financial information. In this study, the microgrid planning problem is broken down into

an investment problem and an operation subproblem. The optimality of the solution is examined by employing the optimal planning decisions obtained from the master problem in the subproblem under uncertain conditions. The study in [18] proposes an operation planning model considering load/generation changes for a low voltage DC microgrid including DC sources such as battery, fuel cell, and PVs. The objective of the study is to minimize daily operation costs. The model utilizes a multi-path dynamic programming approach to solve the problem. In [19], a two-layer control scheme is proposed for improving the economic operation of islanded hybrid AC/DC microgrids. At the lower layer, an iterative solution for the decentralized dispatch in real time is presented to ensure the simultaneous implementation of the decentralized economic dispatch and frequency/voltage regulations in each section. At the upper layer, the operation of AC and DC sections is coordinated by regulating the interlinking converters power exchange. The study in [20] proposes the concept of a transfverter inspired by how transformers link ac grids to address challenges of stiff voltage sources in AC or DC subgrids in designing interlink converters between AC and DC subgrids. In [21], a distributed architecture for robust and optimal control of DC microgrids with a network of multiple DC-to-DC converters is proposed. The study in [22] presents an optimal energy-emission management in hybrid AC-DC microgrids with vehicle-2-grid technology. This model is proposed as a constrained multi-objective problem which optimizes both cost and emission objectives. An effective optimization solution called the theta-crow search algorithm is developed to cope with the problem complication and nonlinearity. In the presence of various renewable DGs, robust controllers are required to ensure good power quality and regulate grid voltage. In [23], these challenges are

addressed by proposing a fixed frequency sliding mode control of renewable energy resources in DC microgrids. The study in [24] proposes an optimal and robust control approach in DC microgrids in which trajectory tracking for nonlinear systems is achieved. The trajectory tracking approach in power converters' control is suitable for harmonics compensation/reduction, power factor correction, and sinusoidal voltage/current restoration.

The study in [25] presents a multi-objective optimal scheduling of a DC microgrid consisting of a PV system and an electric vehicle charging station. In this study, the cost of electricity and energy circulation of storage are taken as objective functions, and the mathematical model is built and solved to obtain the Pareto optimal solution. The study in [26] investigates a control system for hybrid AC/DC microgrids connected by multi-level inverters. The droop control technique is offered to manage power flows between AC microgrid, DC microgrid, and the main grid. The study in [27] discusses the power management in a hybrid AC/DC microgrid and proposes an interlinking AC-to-DC converter accompanied by a suitable control system. The power flow between different sources throughout both microgrids is controlled. The hybrid AC/DC microgrid allows different loads and DERs connect with the minimum need for electrical conversion, which decreases the cost and energy losses. The study in [28] states that the efficiency of distributed generations and DESs in a microgrid might reduce because of microgrid operation, hence running some consumers into problem. This study proposes an optimized operation planning for distributed generations and DESs in microgrids to solve this issue. In [29], a model for energy management and operational planning of microgrids with PV-based active generators is presented, which

includes a deterministic energy management system for microgrids composed of PV units, energy storage system, and gas microturbines. The integration of the proposed deterministic energy management method for business customers in the microgrid is further discussed.

1.4 Hybrid AC/DC Microgrid Planning

Hybrid microgrids provide the opportunity to combine the benefits of both AC and DC microgrids. In hybrid microgrids, AC loads and DERs could be connected to AC buses, and DC loads and DERs could be connected to DC buses. Therefore, the number of the required converters and the associated conversion power losses would be minimized, thus significantly decreasing the planning cost and increasing the energy efficiency. Moreover, the integration of DC DERs would be easier through simplified interfaces compared to connections in AC microgrids. These benefits can introduce hybrid AC/DC microgrids as one of the most viable and desirable options in developing the future power grids. A literature review about existing work on hybrid AC/DC microgrid planning is provided below.

A bi-level planning approach for hybrid AC/DC distribution system considering N-1 security criterion is proposed in [30]. The proposed model consists of two levels. The upper-level model optimizes the total investment and operation costs in both AC and DC system over the planning horizon. The lower-level model aims at improving the DC system's reliability by minimizing curtailment cost of wind and solar under the worst N-1 contingency. In [31], a planning model for hybrid AC/DC microgrids is proposed which takes into account the line factors for the distributed power capacity. The presented model integrates a number of factors, such as power investment costs,

line expansion, and load reliability. The study in [32] proposes an optimal configuration of hybrid AC/DC urban distribution networks for high penetration renewable energy. The proposed model consists of two levels. In the upper level, a multiple objective optimal model is proposed to balance investments, power losses, and the maximum load level and renewable energy capacity. In the lower level, daily operations of the installed voltage source converters are optimized by a chance constraint programming.

The study in [33] investigates the optimal planning and design of a hybrid microgrid which aims at minimizing the total planning cost by considering environmental issues such as carbon emissions. In order to assess the economical and operational performance of the proposed model, various DER mixes are compared. In [34], a comprehensive review on AC and DC technology in microgrids is provided and various parameters, features, advantages, and disadvantages of each technology type are discussed. It is explained that DC technology has several advantages over AC technology specifically for long distances. For example, DC lines are associated with lower losses and higher transmit power. On the other hand, DC protection systems are more expensive than AC systems. It is stated that although HVDC installations have been increasing due to the advantages of the DC technology, most microgrids still use the AC technology as there is a need for more research on islanding control techniques and standardization of DC systems. At the end, it is specified that hybrid AC/DC microgrids could be more practical than dc microgrids. In [35], two main groups of hybrid microgrids have been identified: coupled AC and decoupled AC configurations. The coupled AC configuration includes two approaches of the completely-isolated and partially-isolated topologies. It is shown that the topology with a full-size power

transformer and an AC-to-DC converter has a smaller size and better performance compared to the other one. As of the decoupled AC configuration, the three-stage converter topology is proved to have several advantages in terms of an easier integration of various devices and providing a full power control over the network. In [36], microgrid uncertainties are considered to design a fault tolerant predictive control mechanism for a reliable energy management by ensuring the availability of the required energy in storage systems. This study is an extension of a model predictive control approach which considers power consumption, energy constraints, and multiple sources of uncertainties associated with variations in the environment, such as the wind speed, solar irradiance, load, and electricity market price changes. In [37], a microgrid planning problem with the objective of determining the optimal size and type of distribution generations (DGs) to be installed with combined heat and power (CHP) systems is studied. The model aims at simultaneously minimizing the total planning cost and carbon dioxide emissions. The problem is solved using multi-objective genetic algorithm. It is assumed that the microgrid operates in the grid-connected mode to be able to buy/sell power from/to the utility grid. It is shown that the installation of thermal storage would significantly improve the system performance by compensating the fluctuations and intermittency of the power generated by renewable DGs. In [38], a model for the integration of renewable DGs in hybrid AC/DC microgrids is proposed. In this model, an additional dc power line is considered in the microgrid as the point of connection of renewable DGs. A thorough review of various control schemes and power management strategies of hybrid AC/DC microgrids under both steady-state and transient conditions is proposed in [39]. In [40], the impact of location and load on

microgrid design is studied, where 96 different combinations of location and load profiles are tested for a planning period of 20 years. The considered DGs include solar PV, wind turbine, microturbine, thermal storage, and a battery bank. The artificial neural network has been used to predict the relative cost, emissions, and renewable penetration in the microgrid optimal design. The results show how the optimal design is different for microgrids serving commercial loads. The necessity of coordination between the distributed load and generation in microgrids by enhancing the system controllability, flexibility, energy management, and storage capability is studied in [41]. The work further implements a real-time optimal power flow management on a real hybrid smart microgrid.

1.5 Co-Optimization Generation and Distribution Planning in Microgrids

One important issue in distribution lines is power congestion. Congestion in distribution lines or disturbance in the upstream utility grid may prevent fully supplying the loads in a distribution network. Moreover, addition of new loads to the network may require timely upgrade of the existing distribution network assets. An efficient distribution planning is required in this case to cope with the potential network problems. There are various methodologies proposed in the literature for distribution network planning. In [42], a methodology for optimal expansion planning of distribution networks is presented which considers network contingencies and relocation of switchgears. The optimization methodology consists of two stages in which the investment and operation problems are solved in the first and second stages, respectively. The study in [43] proposes an algorithm to capture the load variations along with the generation volatility and intermittency of renewable energy sources. The

proposed model coordinates voltage control among smart grid technologies by determining the optimal number of DG units. In [44], a model for distribution grid planning enhancement is presented using profiling estimation technique. The objective of the proposed model is to reconstruct the load profile of the medium/low voltage substations. The study in [45] proposes a methodology to be used by distribution system operators (DSOs) for optimal distribution grid planning. The proposed model can be used in meshed and radial grids. Both passive and active network measures are considered in this study. The solution of this model determines whether a new line or transformer should be installed or any other reinforcement actions should be taken. In [46], the economic impact of demand response on distribution network planning is investigated. The reference network model, a large-scale distribution network planning tool, is used to take appropriate action in response to demand growth in a ten-year planning horizon. The study in [47] presents the microgrid planning as an alternative to generation and transmission expansion. The microgrid-based co-optimization planning problem is solved by decomposition to a planning problem and annual reliability subproblem.

The rest of the dissertation is organized as follows. A model for AC versus DC microgrid planning is proposed in Chapter Two, in which only individual AC or DC microgrids are considered. Chapter Three introduces hybrid AC/DC microgrids as a more economical solution compared to individual AC or DC microgrids. Chapter Four presents a co-optimization generation and distribution planning in microgrids aiming at minimizing the microgrid long-term operation cost while ensuring a reliable supply of loads. In this research, power flow is modeled, and respective equations are linearized

using minor approximations in order to be able to formulate the problem using mixed integer linear programming (MILP). Further, this chapter proposes a preprocessing approach to identify uncertainties in the microgrid that result in the robust (i.e., worst-case) solution. All the proposed models are tested on a test microgrid to show their merit and effectiveness.

2. Chapter Two: AC Versus DC Microgrid Planning

A model for AC versus DC microgrid planning is proposed in this chapter [48]. It is assumed in this study that the microgrid developer is planning to deploy a microgrid, however, the challenge is to determine the type of the microgrid, i.e., either AC or DC, based on the system characteristics and accordingly determine the optimal DER generation mix. This study aims at proposing a microgrid planning model with the overarching goals of i) Determining the optimal DER generation mix; ii) Determining the optimal type of the microgrid, i.e., either AC or DC, from an economic perspective; and iii) Identifying threshold ratios of DC loads which make the DC microgrid a more economically viable alternative than the AC microgrid. This chapter is limited to the modeling of individual AC and DC microgrids, and the hybrid AC/DC microgrid planning model is investigated in Chapter Three. The proposed microgrid planning model minimizes the total planning cost associated with the investment costs of DERs, AC-to-DC rectifiers, and DC-to-AC inverters, as well as the microgrid operation and reliability costs.

The investment cost is typically higher for DERs compared to conventional energy resources within large-scale power plants due to economies-of-scale of the latter. Nevertheless, DERs could provide less expensive energy in comparison with the energy purchased from the main grid specifically during peak hours when the market price is high. The DES could be further employed to be charged by the power from the main

grid during low-price hours and discharged during high-price hours. One important and salient feature of microgrids that increases the reliability is their islanding capability which allows microgrids to be disconnected from the main grid in the presence of faults, disturbances, or voltage fluctuations in the upstream network. However, if after disconnecting from the main grid the microgrid could not supply all the loads, some loads should be curtailed, but critical loads will still be supplied. Another economic benefit of the microgrid is selling back the excess power to the main grid. The microgrid economic viability is ensured when the total microgrid revenue from all available value streams in a specified time horizon exceeds the microgrid total investment cost. The total planning cost is comprised of three parts: the investment cost, the operation cost, and the reliability cost. The investment cost is long-term and calculated annually while the operation and reliability costs are short-term and should be calculated hourly for each day of the planning horizon.

2.1 Model Outline

In reality, several components should be considered to install the microgrid, but only the investment cost of DERs, rectifiers and inverters are included in this study. Other costs associated with distribution network upgrade and installation of additional transformers, switches, measurement devices, and controllers are ignored in this study since these costs will be similar in both types of the microgrid. A general structure of DC microgrids is shown in Fig. 2.1. In DC microgrids, three-phase AC-to-DC rectifiers and transformers are required to connect AC DERs to the common bus, single- and three-phase DC-to-AC inverters are needed for supplying AC loads, and a three-phase

DC-to-AC/AC-to-DC converter, a transformer, and a point of common coupling switch are required for connecting the microgrid to the utility grid.

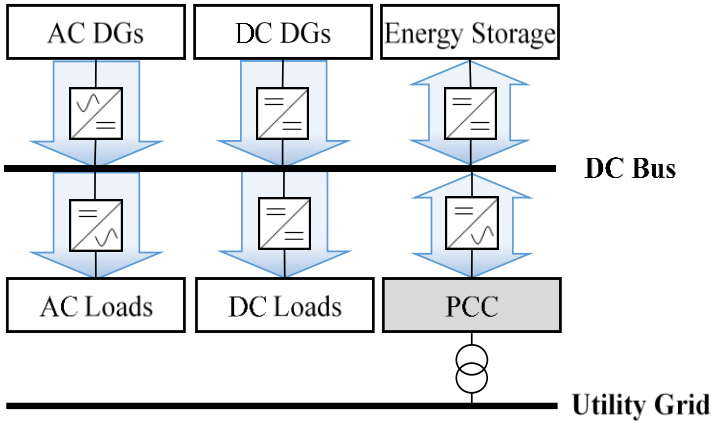

Fig. 2.1 General structure of DC microgrids

A general structure of AC microgrids is shown in Fig. 2.2. In AC microgrids, three-phase DC-to-AC inverters are required to connect DC DERs to the common bus, three-phase AC-to-DC rectifiers are needed for supplying DC loads, and similar to DC microgrids, a transformer and a point of common coupling switch are required to connect the microgrid to the utility grid. The direction of arrows in Figs. 2.1 and 2.2 shows the direction of power flow. It should be noted that different DC loads require different DC voltage levels, so some DC-to-DC converters have to be considered as well in order to change the voltage level of the DC sources to desired levels. In both microgrids, a common bus is considered to show all the connections of loads and DERs. In reality, however, the common bus could represent one or more loop/radial distribution networks that connect loads and DERs within the microgrid. In DC microgrids the common bus would handle DC voltages and currents, while in AC microgrids the common bus would be used for AC voltages and currents.

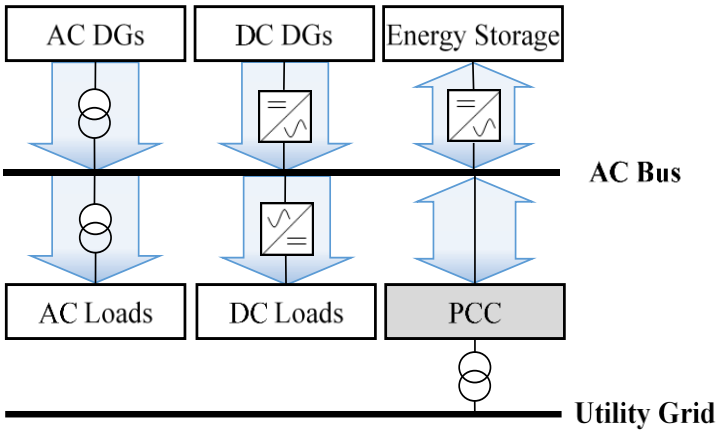

Fig. 2.2 General structure of AC microgrids

The capacity of lines in a microgrid distribution network is typically much higher than the power transferred through the lines, therefore, the power flow is not considered in the proposed planning problem as the congestion is less likely and would not impact the planning results. Moreover, although the proposed planning model can be extended to include hybrid microgrids, it is limited in this chapter to the modeling of AC and DC microgrids. The hybrid microgrid planning problem will be investigated as a follow-on work.

2.2 Problem Formulation

The objective of the microgrid planning problem is to minimize the microgrid total planning cost (2.1), which comprises the investment cost of DERs, rectifiers, and inverters (*IC*), the microgrid operation cost (*OC*), and the reliability cost (*RC*). The investment, operation, and reliability costs are determined in (2.2)-(2.5). Associated constraints are defined in (2.6)-(2.17). The type of the microgrid, i.e., either AC or DC, would impact the components to be installed in the microgrid, and accordingly, alter the investment cost. Constraints (2.2) and (2.3) respectively define the DC investment cost

and the AC investment cost, based on a binary decision variable z. If the microgrid is DC, the binary decision variable is set to one, relaxing (2.3), and the investment cost would be determined by (2.2). Similarly, if the microgrid is AC, the binary decision variable is set to zero, relaxing (2.2), and the investment cost would be determined by (2.3).

$$\min IC + OC + RC \tag{2.1}$$

$$-M(1-z) \le IC - \left(\begin{array}{l} \sum_t \sum_{i\in\{\mathrm{G,W}\}} \kappa_t CC_{it} P_i^{\max} + \\ \sum_t \sum_{i\in\mathrm{S}} \kappa_t (CP_{it} P_i^{\max} + CE_{it} C_i^{\max}) + \\ \sum_t \sum_{i\in\{\mathrm{G_{ac},W_{ac}}\}} \kappa_t CR_{it} P_i^{\max} + \\ \sum_t \sum_{i\in\mathrm{I}} \kappa_t CI_{it} (1-\alpha).\max(PD_{bht}) + \\ \sum_t \sum_{i\in\mathrm{I}} \kappa_t CI_{it} P_M^{\max} \end{array} \right) \le M(1-z) \tag{2.2}$$

$$-Mz \le IC - \left(\begin{array}{l} \sum_t \sum_{i\in\{\mathrm{G,W}\}} \kappa_t CC_{it} P_i^{\max} + \\ \sum_t \sum_{i\in\mathrm{E}} \kappa_t (CP_{it} P_i^{\max} + CE_{it} C_i^{\max}) + \\ \sum_t \sum_{i\in\{\mathrm{G_{dc},W_{dc},E}\}} \kappa_t CI_{it} P_i^{\max} + \\ \sum_t \sum_{i\in\mathrm{R}} \kappa_t CR_{it} \alpha.\max(PD_{bht}) \end{array} \right) \le Mz \tag{2.3}$$

$$OC = \sum_t \sum_h \sum_b \sum_{i\in\mathrm{G}} \kappa_t c_i P_{ibht} + \sum_t \sum_h \sum_b \kappa_t \rho_{bht} P_{M,bht} \tag{2.4}$$

$$RC = \sum_t \sum_h \sum_b \kappa_t v_{bht} LS_{bht} \tag{2.5}$$

AC and DC microgrids have some similar components in the investment cost. The first two terms within the investment cost in (2.2) and (2.3) indicate the investment cost of DGs and DES, respectively. The investment cost of DERs depends on their installed power capacity which will be determined by the optimization problem. The

investment cost of DES further depends on its installed energy capacity. A single-step price curve is considered for DERs, which could be simply extended to a multi-step price curve. If the microgrid is DC, the output voltage of AC generating units should be converted to DC using rectifiers. Therefore, another term that should be considered is related to the investment cost of AC-to-DC rectifiers. Additionally, there are AC loads in the microgrids requiring the use of DC-to-AC inverters. As a result, the investment cost of these inverters is included in the investment cost. The last term of the investment cost considers the DC-to-AC inverter which is used for connecting the DC microgrid to the utility grid. For AC microgrids, as proposed in (2.3), DC-to-AC inverters have to be used for connecting DC units to the microgrid, and AC-to-DC rectifiers are needed for supplying DC loads. These costs are included in the investment cost as well.

The operation cost (2.4) includes the generation cost of dispatchable generating units and the cost of energy purchase from the main grid, which is defined as the amount of purchased energy times the market price at the point of common coupling. If the microgrid is exporting its excess power to the main grid, the main grid power P_M would be negative (assumed to be paid at the market price under net metering); hence, there would be a benefit from selling the excess power. On the other hand, if there is a need for importing power from the main grid, P_M would be positive, increasing the operation costs. The reliability cost (2.5), which is the cost of unserved energy, is defined as the load curtailment quantity multiplied by the value of lost load (VOLL). VOLL represents customers' willingness to pay for reliable electricity service in order to avoid outage. VOLL highly depends on sector or customer type, timing of outage, duration of outage, and time of advanced notification of outage and preparation. Generally, VOLL for

residential customers ranges from approximately \$0/MWh to \$17,976/MWh, while for commercial and industrial customers ranges from \$3,000/MWh to \$53,907/MWh [49]. Higher VOLLs represent more critical loads [50][51]. A discount rate *r* is considered in order to evaluate the objective in terms of discounted costs. The present-worth cost component κ_t is present in all parts of the cost function which is calculated as $\kappa_t = 1/(1+r)^{t-1}$. In (2.1)-(2.4), investment costs are calculated annually while operation and reliability costs are calculated hourly and summed over all the years in the planning horizon.

Islanding is the most salient feature of microgrids, which enables the microgrid to be disconnected from the main grid in case of upstream network disturbances. In order to include the islanding ability of the microgrid, it is required to consider a condition to make sure that dispatchable generation capacity installed in the microgrid is adequate to seamlessly supply critical loads (2.6). The parameter β defines the peak ratio of critical loads to total loads.

$$\beta.PD^{\max} \leq \sum_{i \in G} P_i^{\max} \tag{2.6}$$

Sum of the power from the main grid and from all DERs, including dispatchable and nondispatchable units as well as DES, should be equal to the total load in each scheduling hour. Equations (2.7) and (2.8) consider the power balance equation in DC and AC microgrids, respectively. If the microgrid is DC, the binary decision variable is set to one, thus (2.8) would be relaxed, and (2.7) would be applied. Similarly, if the microgrid is AC, (2.7) would be relaxed and (2.8) would be applied.

$$-M(1-z) \le \left(\begin{array}{l} \sum_{i\in\{G_{dc},W_{dc}\}} P_{ibht} + \sum_{i\in E}(P^{dch}_{ibht} - P^{ch}_{ibht}) + \\ \left(\sum_{i\in\{G_{ac},W_{ac}\}} P_{ibht} + P_{M,bht} \right).\eta_{rec} \\ +LS_{bht} - \alpha.PD_{bht} - \dfrac{(1-\alpha).PD_{bht}}{\eta_{inv}} \end{array} \right) \le M(1-z) \qquad \forall b, \forall h \tag{2.7}$$

$$-Mz \le \left(\begin{array}{l} \sum_{i\in\{G_{ac},W_{ac}\}} P_{ibht} + \\ \left(\sum_{i\in\{G_{dc},W_{dc}\}} P_{ibht} + \sum_{i\in E}(P^{dch}_{ibht} - P^{ch}_{ibht}) \right).\eta_{inv} + \\ P_{M,bht} + LS_{bht} - (1-\alpha).PD_{bht} - \dfrac{\alpha.PD_{bht}}{\eta_{rec}} \end{array} \right) \le Mz \qquad \forall b, \forall h \tag{2.8}$$

In DC microgrids, since power conversion causes power loss, an efficiency coefficient is defined in (2.7) for AC-to-DC rectifiers, used for converting the output of AC generating units and the power from the main grid, and for DC-to-AC inverters, used for supplying AC loads. Similar efficiency coefficients are considered for the AC microgrid (2.8).

The planning problem is further subject to constraints associated with the main grid power limits (2.9), dispatchable and nondispatchable unit operation and planning (2.10)-(2.12), DES (2.12)-(2.16), and load curtailment (2.17).

$$-P^{\max}_{M} u_{M,bht} \le P_{M,bht} \le P^{\max}_{M} u_{M,bht} \qquad \forall b, \forall h \tag{2.9}$$

$$0 \le P_{ibht} \le P^{\max}_{i} \qquad \forall i \in \mathrm{G}, \forall b, \forall h \tag{2.10}$$

$$P_{ibht} = P^{\max}_{i} . \zeta_{ibht} \qquad \forall i \in \mathrm{W}, \forall b, \forall h \tag{2.11}$$

$$P^{\max}_{i} \le P^{cap}_{i} \qquad \forall i \in \{\mathrm{G,W,E}\} \tag{2.12}$$

$$0 \le P^{dch}_{ibht} \le P^{\max}_{i} \qquad \forall i \in \mathrm{E}, \forall b, \forall h \tag{2.13}$$

$$0 \le P_{ibht}^{ch} \le P_i^{\max} \qquad \forall i \in \mathrm{E}, \forall b, \forall h \tag{2.14}$$

$$C_i^{\max} \le C_i^{cap} \qquad \forall i \in \mathrm{E} \tag{2.15}$$

$$0 \le \sum_{k \le b} (P_{ikht}^{ch} - P_{ikht}^{dch} / \eta_i) \le C_i^{\max} \quad \forall i \in \mathrm{E}, \forall b, \forall h \tag{2.16}$$

$$0 \le LS_{bht} \le PD_{bht} \qquad \forall b, \forall h \tag{2.17}$$

The amount of exchanged power with the main grid is limited by the capacity of the line connecting the main grid to the microgrid (2.9). In (2.9), the islanding capability of the microgrid is considered by defining a binary parameter which controls microgrid islanding. The power generated by dispatchable units is limited by their installed capacity (2.10). For nondispatchable units, a variable and a parameter are used to consider their generation. Similar to dispatchable DGs, the variable P_i^{max} represents their installed capacity, which will be determined via the optimization problem. The parameter ζ_{ibht} represents the normalized generation forecast of nondispatchable DGs and has a value between 0 and 1 (2.11). Once a forecast is obtained, it is divided by the rated power of the candidate DER, hence, the normalized generation forecast is obtained. In this case, the selected size of the nondispatchable DG will be considered as a scaling factor to scale up/down the normalized generation forecast and further obtain the actual generation. All DERs have an allowable installation capacity, and their installed capacity cannot exceed this limit (2.12). The allowable installation capacity may be obtained from budget limitations, choice of technology, or space limitations. The DES charging and discharging power in all hours is limited by its installed capacity (2.13)-(2.14). The DES installed energy capacity is limited by its allowable installation energy capacity (2.15). Additionally, its stored energy is determined based on the net

charged power, efficiency, and the stored energy in previous hours (2.16). It is further ensured that in case of local curtailments, the hourly curtailed load does not exceed the hourly total load (2.17).

2.3 Numerical Simulations

A microgrid is to be installed for a group of electricity customers with a peak annual load demand of 8.5 MW. The set of DERs used in this study includes four AC dispatchable units, one AC nondispatchable unit (wind generator), one DC nondispatchable unit (solar PV), and one DES, as represented in Tables 2.1-2.3. The cost of converters is provided in Table 2.4. The load, renewable energy, and market price are forecasted based on historical data obtained from the Illinois Institute of Technology Campus Microgrid [52]. Data of wind, solar, and converters are gathered from [53][54][55]. The DES efficiency and VOLL are considered to be 90% and $10,000/MWh, respectively. The planning horizon is 20 years. The lifetime of candidate DERs is considered to be equal to the planning horizon, i.e., 20 years. Twelve hours of islanding is considered in each planning year. The microgrid planning problem was implemented on a high-performance computing server consisting of four 10-core Intel Xeon E7-4870 2.4 GHz processors. The problem was formulated by mixed-integer programming (MIP) and solved by CPLEX 12.6 [56]. Following cases are studied. The approximate running time for each simulation is 118-155 minutes.

Case 0: Base case microgrid planning

Case 1: Sensitivity analysis on the ratio of DC loads

Case 2: Sensitivity analysis on the ratio of critical loads

Case 3: Sensitivity analysis on the efficiency of AC-to-DC rectifiers and DC-to-AC inverters

Case 4: Sensitivity analysis on the market price

Table 2.1 Dispatchable Units Characteristics

Unit Number	Type	Allowable installation capacity (MW)	Cost Coefficient ($/MWh)	Annualized Investment Cost ($/MW)
1	Gas	5	90	50,000
2	Gas	5	90	50,000
3	Gas	3	70	70,000
4	Gas	3	70	70,000

Table 2.2 Nondispatchable Units Characteristics

Unit Number	Type	Allowable Installation Capacity (MW)	Cost Coefficient ($/MWh)	Annualized Investment Cost ($/MW)
5	Wind	2	0	132,000
6	Solar	2	0	133,000

Table 2.3 DES Characteristics

Allowable Installation Capacity (MW)	Allowable Installation Energy (MWh)	Annualized Investment Cost – Power ($/MW)	Annualized Investment Cost – Energy ($/MWh)
1	6	60,000	30,000

Table 2.4 Annualized Investment Cost of Converters

Three-Phase AC-to-DC Rectifier ($/MW)	Single-Phase DC-to-AC Inverter ($/MW)	Three-Phase DC-to-AC Inverter ($/MW)
4,200	6,000	6,500

Case 0: Initial values for the ratio of DC loads α, the ratio of critical loads β, and the efficiency of inverters and rectifiers η, are chosen to be 0.40, 0.50, and 0.70, respectively. The microgrid planning solution would install dispatchable units 3 and 4 and the solar unit all with the maximum allowable capacity. The planning solution would be the AC microgrid. The total planning cost in the base case is $25,608,640 with

a cost breakdown of $6,679,653, $18,614,730, and $314,251 for the investment, operation, and reliability costs, respectively.

Case 1: In this case, the effect of changing the ratio of DC loads α on the type of the microgrid and installation of DERs is studied. The ratio of DC loads is changed by a step of 0.1 while all other parameters are kept unchanged. Results are represented in Tables 2.5 and 2.6. For values of α between 0 and 0.4, the microgrid planning solution would install dispatchable units 3-4 and the solar unit, while by changing α between 0.5-0.8, dispatchable units 1 and 2 are also installed. However, for α=0.9 and 1, units 1 and 2 are not installed anymore, and the microgrid planning solution would install the DES since the type of the microgrid is DC. The obtained results advocate that the installation of dispatchable units 3 and 4 with a higher investment cost is more economical than that of units 1 and 2. The reason is that units 3 and 4 offer a less expensive power compared to units 1 and 2. Additionally, between the two available nondispatchable units, the solar unit is installed for all values of α although it has a higher investment cost than the wind unit since the generation pattern of the solar unit partially coincides with market price and load variations. The daily values of load, solar generation, and market price, averaged over one year, are shown in Fig. 2.3 to demonstrate the partial correlation of the solar generation with the market price and the load. According to Fig. 2.3, during the day, especially at peak hours, the market price is higher, and the solar unit generates power. Therefore, part of loads could be supplied by solar generation. On the other hand, the wind energy is available mostly at early morning hours, when the market price is relatively low. As expected, according to results and based on the values of β and η, increasing the ratio of DC loads causes the microgrid to

shift from AC (associated with z=0) to DC (associated with z=1). According to Table 2.6, by increasing α from 0.4 to 0.8, the microgrid investment cost increases because of increasing the installed capacity of units 1 and 2 and also increasing the investment cost of rectifiers for supplying DC loads. For values of α between 0.4 and 0.8, the operation cost would increase as well since the amount of hourly power generated by dispatchable units 1 and 2 increases. By increasing α from 0.8 to 0.9, again the investment cost rises due to the installation of the DES, but the operation cost would decrease since units 1 and 2 are not installed anymore. The investment and operation costs would decrease by increasing α from 0.9 to 1. The investment cost drops as there are not any AC loads in the microgrid when α=1, thus the investment cost of inverters is eliminated. The operation cost drops as the overall exchanged power with the main grid decreases by changing all loads to DC. Accordingly, the microgrid total planning cost would decrease by increasing α from 0.9 to 1. An interesting point is the change in the total planning cost by changing the load mixture. According to Table 2.6, increasing the ratio of DC loads would cause an increase followed by a decrease in the total planning cost. Therefore, it would identify threshold ratios of DC loads which make the DC microgrid a more economically viable solution than the AC microgrid. In other words, for ratios smaller than the threshold ratio, AC microgrid would be more economical and for ratios larger than that, DC microgrid would be more economical.

Table 2.5 Installed DER Capacity (MW) with Respect to Ratio of DC Loads

Ratio of DC Loads	Microgrid Optimal Type	DER								
		1	2	3	4	5	6	7	DES	
									P	E
0.00- 0.40	AC	0	0	3.0	3.0	0	0	2.0	0	0
0.50	AC	0.03	0.03	3.0	3.0	0	0	2.0	0	0
0.60	AC	0.15	0.15	3.0	3.0	0	0	2.0	0	0
0.70	AC	0.27	0.27	3.0	3.0	0	0	2.0	0	0
0.80	AC	0.40	0.40	3.0	3.0	0	0	2.0	0	0
0.90, 1.00	DC	0	0	3.0	3.0	0	0	2.0	1.0	4.44

Table 2.6 Microgrid Costs with Respect to Ratio of DC Loads

Ratio of DC Loads	Investment Cost ($)	Operation Cost ($)	Reliability Cost ($)	Total Cost ($)
0.40	6,679,653	18,614,730	314,251	25,608,634
0.50	6,740,727	19,514,640	359,810	26,615,177
0.60	6,888,104	20,372,440	370,847	27,631,391
0.70	7,035,482	21,230,250	381,884	28,647,616
0.80	7,182,860	22,088,070	392,922	29,663,852
0.90	9,736,027	20,640,090	247,109	30,623,226
1.00	9,688,322	19,335,080	190,476	29,213,878

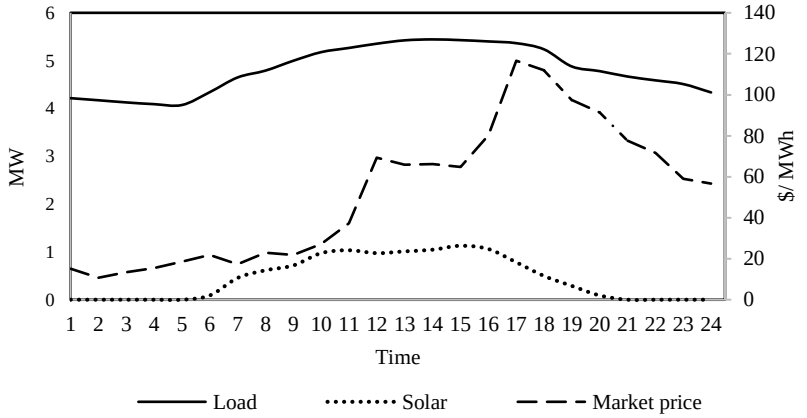

Fig. 2.3 Annual average value of load and solar generation (MW), and the market price ($/MWh) for 24 hours

Case 2: In this case, the effect of changing the ratio of critical loads β on planning results is studied. Results are represented in Tables 2.7 and 2.8. The microgrid planning solution would be the AC microgrid for all values of β. It is reasonable that by keeping α constant, there is not a shift from the AC microgrid to the DC microgrid. The impact of β, however, could be noticed on the installed generation mix. According to Table 2.7, when the value of β is between 0.1 and 0.7, the microgrid planning solution would install dispatchable units 3 and 4 and the solar unit. By increasing the ratio of critical loads to 0.8 and more, units 1 and 2 are also installed, and their installed capacity would increase in order to supply critical loads. Similar to Case 1, the solar unit is always installed due to the coincidence of its generation pattern with the load and market price variations. According to Table 2.8, the operation and reliability costs would decrease by increasing β. Increasing the ratio of critical loads would cause an increase in the total installed DER capacity, while the total load has not changed. As a result, the excess power would be sold to the main grid, which would increase the revenue of the microgrid thus decreasing the operation cost. On the other hand, by increasing the ratio of critical loads, the additional available dispatchable capacity would fully supply loads during islanding events, which causes load curtailments to decrease. Specifically, if all loads are considered as critical (associated with β=1.0), the microgrid planning solution would install more dispatchable capacity so as to fully supply all loads which causes load curtailments to reach zero in expense of a higher investment cost.

Table 2.7 Installed DER Capacity (MW) with Respect to Ratio of Critical Loads

Ratio of Critical Load	Microgrid Optimal Type	DER								
		1	2	3	4	5	6	7	DES	
									P	E
0.10- 0.70	AC	0	0	3.0	3.0	0	0	2.0	0	0
0.80	AC	0.40	0.40	3.0	3.0	0	0	2.0	0	0
0.90	AC	0.82	0.82	3.0	3.0	0	0	2.0	0	0
1.00	AC	1.25	1.25	3.0	3.0	0	0	2.0	0	0

Table 2.8 Microgrid Costs with Respect to Ratio of Critical Loads

Ratio of Critical Load	Investment Cost ($)	Operation Cost ($)	Reliability Cost ($)	Total Cost ($)
0.10-0.70	6,679,653	18,614,730	314,251	25,608,634
0.80	7,050,504	18,433,520	165,911	25,649,935
0.90	7,448,045	18,238,630	76,485	25,763,160
1.00	7,845,585	18,043,630	0	25,889,215

Case 3: In this case, the effect of changing the efficiency of inverters and rectifiers η, which are considered to be equal, on planning results is studied. Results show that changing converters efficiencies while other parameters are kept unchanged would not affect either the type of the microgrid or installed DER mix. According to Table 2.9, the significant impact of changing η would be on the operation and reliability costs. By increasing η, there would be less power loss in inverters and rectifiers. Therefore, the importing power from the main grid in many operation hours would decrease, which causes a reduction in the total operation cost. On the other hand, because of the reduced power loss in converters, more critical loads could be supplied by increasing the efficiency. Accordingly, there would be a reduction in the load

curtailment which reduces the reliability cost. Since the installed power of all DERs is unchanged, the investment cost for different values of η would not change.

Table 2.9 Microgrid Costs with Respect to Converters' Efficiency

Converters' Efficiency	Investment Cost ($)	Operation Cost ($)	Reliability Cost ($)	Total Cost ($)
0.70	6,679,653	18,614,730	314,251	25,608,634
0.80		16,695,660	204,170	23,579,483
0.90		15,114,700	144,303	21,938,656
1.00		13,770,440	114,252	20,564,345

Case 4: In this case, the effect of changing the market price ρ on planning results is studied. The installed power of DERs and costs associated with different market prices are represented in Tables 2.10 and 2.11, respectively. By 10% decrease in the market price, the microgrid planning solution remains unchanged, except for the installed capacity of dispatchable units 3 and 4. Generally, when the market price is low, the microgrid would buy more power from the main grid, hence the exchanged power with the main grid would be positive in many hours. Therefore, the power generation of DERs would decrease in several hours, which reduces the operation cost. Increasing the market price by 10% causes the microgrid planning solution to install DERs 1 and 2 in addition to DERs 3, 4, and 7, thus the investment cost would decrease. By increasing the market price by 20% or more, the microgrid should generate more power in several hours in order to supply loads, and on the other hand, it would be desirable to sell more electricity to the main grid. Therefore, all AC dispatchable units, wind generator and solar PV would be installed at their maximum capacity, and the exchanged power with the main grid would be negative in several hours. As a result, the operation cost would

decrease due to the revenue from selling more power to the main grid. It is further reasonable that all critical loads be supplied by increasing the total DER capacity. Accordingly, there would not be any load curtailment, which causes the reliability cost to reach zero. Since DER generation mix is the same when there is a 20% or more increase in the market price, the investment cost would not change. Similar to previous cases, the type of the microgrid would remain the same, i.e., AC, since the ratio of DC loads is unchanged.

Table 2.10 Installed DER Capacity (MW) with Respect to Market Prices

Price Change Coefficient	Microgrid Optimal Type	DER								
		1	2	3	4	5	6	7	DES	
									P	E
0.9	AC	0	0	2.91	2.91	0	0	2.0	0	0
Original Price	AC	0	0	3.00	3.00	0	0	2.0	0	0
1.1	AC	1.23	1.23	3.00	3.00	0	0	2.0	0	0
1.2	AC	5.00	5.00	3.00	3.00	0	2.0	2.0	0	0
1.3	AC	5.00	5.00	3.00	3.00	0	2.0	2.0	0	0
1.4	AC	5.00	5.00	3.00	3.00	0	2.0	2.0	0	0

Table 2.11 Microgrid Costs with Respect to Market Prices

Price Change Coefficient	Investment Cost ($)	Operation Cost ($)	Reliability Cost ($)	Total Cost ($)
0.9	6,558,827	17,790,310	348,773	24,697,910
Original Price	6,679,653	18,614,730	314,251	25,608,634
1.1	7,830,468	18,306,340	0	26,136,808
1.2	13,834,450	11,436,000	0	25,270,450
1.3	13,834,450	9,209,981	0	23,044,431
1.4	13,834,450	6,537,612	0	20,372,062

Although in proposed studies, it is assumed that annual changes in load, renewable generation, and market prices are negligible, the proposed microgrid planning model has the capability to efficiently consider respective annual changes. Considering significantly small changes in the load is a practical assumption, perceivably due to the limited geographical boundaries of the microgrid which limits significant load increase as well as the increased adoption of efficiency schemes which helps with load reduction. Also renewable generation would remain the same over the planning horizon as the installed capacity will not change. The market price, however, has the highest possibility to increase. To demonstrate the impact of the market price increase the proposed planning problem is solved for a 2% annual increase in market prices. The total planning cost in this case is reduced to $24,635,350 with a cost breakdown of $9,296,503, $15,239,520, and $99,326 for the investment, operation, and reliability costs, respectively. Following the increase in market prices, the microgrid would be willing to sell more power to the main grid which causes a drop in the operation cost. On the other hand, in order to be able to sell more electricity the microgrid would install additional DER capacity which causes an increase in the investment cost.

Arbitrary values for DERs' allowable installation capacity were used in the proposed studies to show the effectiveness of the microgrid planning model in handling capacity limitations. If the limits are removed, the planning problem will select only the most economical candidate while ignoring all other candidates, which is not a very practical assumption. Some examples of these limitations are the rooftop solar panel installations in a community microgrid, which would be restricted by the rooftop area

that can be covered by panels, and thermal unit, which cannot be installed in densely populated areas.

2.4 Discussions

DC microgrids could potentially improve microgrid economic benefits when the ratio of DC loads is high, and further be considered as viable alternatives to AC microgrid installations. According to the studied cases, following could be concluded:

- Among AC dispatchable generating units, those which offer a less expensive power would be installed first although they may be associated with higher capital costs.
- Among nondispatchable units, the solar unit would be installed in all cases because of the partial coincidence of its generation pattern with the market price and load variations.
- The most decisive factor in determining the type of the microgrid is the ratio of DC loads. Changing this ratio would cause the total cost to change, so it could be used as a tool to find a critical point where DC microgrid would be more economical than the AC microgrid.
- Increasing critical loads, converters efficiency, or the market price would cause a decrease in the operation and reliability costs.
- An increase in critical loads would cause the microgrid planning solution to install more dispatchable capacity which increases the investment cost. Since the total load is unchanged, there would be an excess generated power which would be sold to the main grid, hence the operation cost would decrease. On the other hand, more critical loads would be supplied which causes a decrease in the load curtailment and the reliability cost.

- Increasing converters efficiency would cause a decrease in the power loss which on one hand decreases the importing power from the main grid in many hours, thus decreasing the total operation cost, and on the other hand, more critical loads could be supplied; hence, there would be a reduction in the load curtailment which reduces the reliability cost.
- The investment cost would change by changing the installed DER capacity. Therefore, the investment cost would remain unchanged by increasing η since the DER generation mix does not change.
- By increasing the market price, it would be desirable to install all dispatchable and nondispatchable units in order to sell as much power as possible to the main grid which would cause a decrease in the operation cost, and also supply all critical loads, thus decreasing the load curtailment, and accordingly, the reliability cost.

3. Chapter Three: Hybrid AC/DC Microgrid Planning

3.1 Model Outline

The model proposed for AC versus DC microgrid planning in Chapter Two is extended to consider AC and DC buses/components together as a hybrid AC/DC microgrid [57]. A general structure of hybrid AC/DC microgrid is shown in Fig. 3.1. In AC (DC) microgrids, there are only AC (DC) buses, whereas in a hybrid microgrid, both AC and DC buses exist. A point of common coupling (PCC) switch along with a transformer is required to connect AC and DC buses to the utility grid. The AC bus can be directly connected to the PCC while this connection for the DC bus should be performed using a converter. Various DERs could be used in the microgrid based on the cost, availability, location, and operator preferences. However, the connection of each DER to its associated feeder needs to be done using proper converters. The DC DERs (such as solar PV, fuel cell, DES, etc.) need to be connected to AC feeders using DC-to-AC inverters, and similarly, AC DERs (such as wind turbine, co-gen, etc.) need to be connected to DC feeders using AC-to-DC rectifiers. This is also the case for loads, in which the loads need to be connected to opposite type feeders using proper converters.

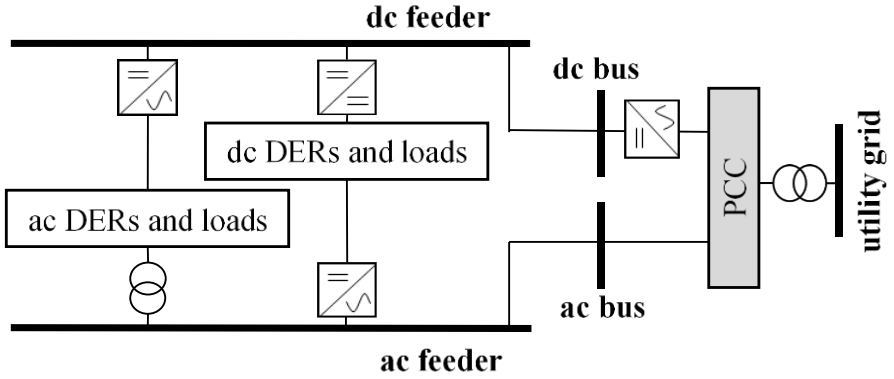

Fig. 3.1 General structure of a hybrid AC/DC microgrid

In this study, both renewable and dispatchable DGs are considered for deployment in the microgrid. Renewable DGs have attracted significant attention in recent years, mainly due to the falling cost of the renewable technology, various economic incentives offered to customers, rapid construction and commissioning, and the ease of installation compared to other types of DGs. Lacking, however, is the generation dispatchability that can ensure an economic and reliable supply of loads in grid-connected and islanded operation modes. Dispatchable DGs, therefore, are deployed in microgrids to ensure a controllable generation and guarantee an economic operation during grid-connected mode and an uninterrupted supply of critical loads during the islanded mode. The DES is further deployed to support renewable generation, enable energy arbitrage to increase economic benefits, and support microgrid control and islanding to increase reliability.

It is assumed in this study that there are a number of feeders while the type of each feeder, i.e., AC or DC, needs to be determined. The decisive factors in determining the type of each feeder include the ratio of AC and DC loads at each feeder and the type of DERs connected to each feeder, which would accordingly impact the investment cost. Considering that the capacity of lines in a microgrid distribution network is typically

much higher than the power transmitted through the lines, the congestion would be less likely to occur. Therefore, the microgrid distribution network power flow and associated line limits are not considered in the proposed planning problem as they would not affect the planning results.

3.2 Problem Formulation

The objective of the hybrid microgrid planning problem is to minimize the total planning cost (3.1), similar to what was discussed in Chapter two. In (3.1), each of the investment, operation, and reliability costs is expressed as the sum of the costs in each planning year. These costs are further explained in detail in (3.2)-(3.4), which are different from those explained in Chapter two, in that the type of each feeder and the point of connection of DERs to feeders should be determined.

$$\min \sum_{t} \kappa_t \left(IC_t + OC_t + RC_t \right) \tag{3.1}$$

$$\begin{aligned} IC_t = & \sum_{k} \sum_{i \in \{\mathrm{G,W,E}\}} CC_{it} P_i^{\max} x_{ik} + CR \sum_{k} \sum_{i \in \{\mathrm{G_{ac}, W_{ac}}\}} P_i^{\max} x_{ik} z_k + CI \sum_{k} \sum_{i \in \{\mathrm{G_{dc}, W_{dc}, E}\}} P_i^{\max} x_{ik} (1 - z_k) \\ & + \sum_{k} \left(CI.\alpha_k{}'.PD^{\max} z_k + CR.\alpha_k.PD^{\max} (1 - z_k) \right) + CI.P_M^{\max} w \qquad \forall t \end{aligned} \tag{3.2}$$

$$OC_t = \sum_{k} \sum_{h} \sum_{b} \sum_{i \in \mathrm{G}} \sum_{q} c_{iq} P_{iqbht} x_{ik} + \sum_{k} \sum_{h} \sum_{b} \rho_{bht} P_{F,kbht} \qquad \forall t \tag{3.3}$$

$$RC_t = \sum_{k} \sum_{h} \sum_{b} v_{bht} LS_{kbht} \qquad \forall t \tag{3.4}$$

The investment cost (3.2) comprises the DER investment cost (first term), and the converter cost (the rest of the terms). The DER investment cost is calculated as the installed power capacity P_i^{max}, which would be determined via the planning problem, times the DER capital cost. For DES, specifically, an additional term associated with the energy investment cost is considered to show the impact of both installed power and

energy capacities (as explained in Chapter two). The investment binary decision variable x_{ik} is further defined and added to the investment cost term to show that, first, whether the DER is installed, and second, determine the feeder to which the DER is connected. In other words, if x_{ik} is obtained as 1 via the planning problem, it means that DER *i* will be installed and will be connected to feeder *k*. The remaining terms in the investment cost represent the cost of converters (both inverters and rectifiers) in the microgrid and are modeled using the binary decision variable z_k. If the microgrid planning solution determines feeder k to be DC, the variable z_k would be set to one, otherwise feeder *k* is AC and z_k would be zero. If a feeder is determined to be DC, the cost of rectifiers used to convert the output of AC DGs should be added. Similarly, if a feeder is determined to be AC, the cost of inverters required to convert the output of DC DGs and DES should be considered in the cost function. The second and third terms in (3.2) address the investment cost of converters. The ratios of DC and AC loads to total loads in each feeder are respectively shown by parameters α_k and $\acute{\alpha_k}$. The fourth term in (3.2) is associated with the cost of inverters and rectifiers required to support voltage conversions for connecting AC and DC loads to DC and AC feeders, respectively. The last term represents the investment cost of the inverter used for connecting DC feeders to the utility grid. A binary decision variable *w* is employed and would be set to one if at least one feeder is DC in the planning problem and set to zero otherwise. This variable would be determined by (3.5) and (3.6). It is assumed that the annualized investment costs of the converters used for all various types of DERs and loads are similar.

$$w \geq z_k \qquad \forall k \qquad (3.5)$$

$$w \le \sum_{k} z_k \tag{3.6}$$

The operation cost (3.3) includes two parts: the generation cost of dispatchable DGs and the cost of energy purchase from the utility grid at all feeders. The former is calculated as the sum of the amount of energy provided by each DG, P_{iqbht}, times its generation price, c_i. For dispatchable DGs, a multi-step price curve is considered. The latter is defined as the sum of the amount of purchased energy at each hour in all feeders, i.e., $P_{F,kbh}$, times the market price ρ_{bht} at the point of common coupling. $P_{F,kbh}$ could be either positive or negative showing that each feeder is acting as a load or a generation.

The reliability cost of each feeder (3.4), which represents the cost of unserved energy, is defined as the amount of load curtailment multiplied by VOLL. There are a number of bilinear terms in the investment cost (3.2) resulting from the multiplication of one continuous and multiple binary variables, which should be linearized in order to obtain a mixed integer programming (MIP) formulation.

The objective function is subject to investment and operation constraints (3.7)-(3.16):

$$\sum_{k} x_{ik} \le 1 \qquad \forall i \in \{\mathrm{G}, \mathrm{W}\} \tag{3.7}$$

$$\beta . PD^{\max} \le \sum_{k} \sum_{i \in \mathrm{G}} P_i^{\max} x_{ik} \tag{3.8}$$

$$\sum_{k} \left(P_{F,kbht} + LS_{kbht} \right) = P_{M,bht} \qquad \forall b, \forall h, \forall t \tag{3.9}$$

Constraint (3.7) is imposed to the planning problem to make sure that each DER is connected to only one feeder. To ensure that the microgrid can seamlessly supply critical loads during islanded operation mode, (3.8) is used. This constraint guarantees that the installed capacity of dispatchable DGs is larger than the peak of critical loads in

the microgrid. The parameter β defines the peak ratio of critical loads to total loads. The microgrid power balance at PCC is ensured by (3.9) in which the sum of transferred power and associated load shedding at all feeders in each hour is equal to the microgrid total exchanged power with the utility grid. If the net exchange power with the utility grid is negative, it means that the microgrid is exporting its excess power to the utility grid, i.e., acting as a generator. However, if the net exchange power with the utility grid is positive, the microgrid acts as a load and imports power from the utility grid.

The feeder load balance constraints are represented by (3.10), where the sum of the power transferred to the feeder with the power from dispatchable and nondispatchable DERs in that feeder equals the total feeder load in each scheduling hour. It should be noted that the power of DES is its net power, obtained by subtracting its power during the charging period from that during the discharging period in each scheduling hour.

$$\sum_{i\in\{G_{ac},W_{ac}\}} P_{ibht}\left(\eta_{rec}z_k+(1-z_k)\right)+\sum_{i\in\{G_{dc},W_{dc},E\}} P_{ibht}\left(z_k+\eta_{inv}(1-z_k)\right)+P_{F,kbht}\left(\eta_{rec}z_k+(1-z_k)\right)=$$
$$\alpha_k{}' PD_{bht}\left(\frac{z_k}{\eta_{inv}}+(1-z_k)\right)+\alpha_k PD_{bht}\left(z_k+\frac{1-z_k}{\eta_{rec}}\right) \qquad \forall k,\forall b,\forall h,\forall t \tag{3.10}$$

The first two terms in (3.10) are associated with the energy delivered by AC and DC DERs in each hour, respectively. If a feeder is DC (associated with $z_k = 1$), AC DERs should be connected via AC-to-DC rectifiers, so an efficiency coefficient is added to consider the power loss in converters. Similarly, if a feeder is AC (associated with $z_k = 0$), DC DERs should be connected via DC-to-AC inverters, so again an efficiency coefficient is added. The third term represents the power transferred to the feeder. A converter is required for exchanging power with the utility grid if at least one feeder is

determined to be DC. The right-hand side of this equation represents AC and DC loads, respectively. The total AC and DC loads in each feeder are calculated as $\alpha_k^{'} PD_{bht}$ and $\alpha_k PD_{bht}$, respectively. In DC feeders, DC-to-AC inverters should be used to supply AC loads, so their efficiencies are considered to calculate losses in power conversion. This is also true for DC loads located in AC feeders which should be connected to their feeder via AC-to-DC rectifiers. The planning problem is further subject to DER and load constraints (2.9)-(2.17).

The linearization method of bilinear terms is explained here. If variable *A* is equal to the multiplication of a continuous variable *B* and *n* binary variables $x_1, x_2, \ldots, x_n$, such as illustrated in (3.11), it can be described by *2(n+1)* constraints as shown in (3.12)-(3.13). *M* is a large positive constant.

$$A = Bx_1x_2x_3\ldots x_n \tag{3.11}$$

$$B - \sum_{i=1}^{n} M(1-x_i) \leq A \leq B + \sum_{i=1}^{n} M(1-x_i) \tag{3.12}$$

$$-Mx_i \leq A \leq Mx_i \qquad \forall i \in \{1,2,\ldots,n\} \tag{3.13}$$

If at least one binary variable is zero, according to (3.13), *A* would be zero, and (3.12) would be relaxed. If all binary variables are one, all *n* constraints in (3.13) would be relaxed, and according to (3.12), *A* would be equal to *B*. Therefore, the equation is linearized, and the results of the constraints defined in (3.12)-(3.13) conform to the original equation in (3.11).

3.3 Numerical Simulations

A microgrid is to be installed for a group of electricity customers with a peak annual load demand of 8.5 MW, similar to what considered in Section 2.3. The set of

DERs used in this study includes four AC dispatchable DGs, one wind generator, one solar PV, and one DES, as represented in Tables 2.1-2.3 in Section 2.3. The annualized investment cost of converters is represented in Table 2.4. Three steps for the power capacity and the cost coefficient of each dispatchable DG are considered as shown in Table 3.1. The load, renewable generation, and market price are forecasted based on the historical data obtained from IIT Campus Microgrid. The VOLL is considered to be $10,000/MWh [48]. It is assumed that the microgrid has three main feeders that their type (AC or DC) needs to be determined. The planning horizon is considered to be 20 years. Twelve hours of islanding is assumed in each planning year, i.e., an average of one hour of islanding in each month. The microgrid planning problem is implemented on a high-performance computing server consisting of four 10-core Intel Xeon E7-4870 2.4 GHz processors. The problem is formulated by MIP and solved by CPLEX 12.6 [56].

Table 3.1 Dispatchable Units Cost Coefficients of Different Steps

Unit Number	Power Generation Capacity (MW)	Cost Coefficient ($/MWh)
1, 2	2	85
	1.5	95
	1.5	105
3, 4	1	65
	1	70
	1	75

Following cases are studied. The approximate computation time for each simulation is between 4 to 10 hours.

Case 0: Base case hybrid microgrid planning

Case 1: Sensitivity analysis on the ratio of DC loads

Case 2: Sensitivity analysis on the ratio of critical loads

Case 3: Sensitivity analysis on the efficiency of AC-to-DC rectifiers and DC-to-AC

inverters

Case 4: Sensitivity analysis on the market price

Case 0: For the base case, initial values for the total ratio of DC loads α, the total ratio of critical loads β, and the efficiency of inverters and rectifiers η, are respectively assumed to be 0.40, 0.50, and 0.70, similar to Section 2.3. The ratio of DC loads to the total DC loads at feeders 1, 2, and 3 is considered to be 39%, 33%, and 28%, respectively. The ratios of AC loads to the total AC loads at feeders 1, 2, and 3 are considered to be 28%, 33%, and 39%, respectively. The ratios of DC loads to the total load in the microgrid in feeders 1, 2, and 3, which are obtained by multiplying the aforementioned ratios by α, is 15.6%, 13.2%, and 11.2%, respectively. It is assumed that all dispatchable DGs can only be installed in feeder 3 (based on space considerations), while the point of connection of renewable DGs and the DES should be determined via the planning problem.

The hybrid microgrid planning solution in this case would install all DGs. Dispatchable units 1 and 2 are installed with a capacity of 0.049 MW and dispatchable units 3 and 4 are installed with a capacity of 2.376 MW. Both wind and solar units are installed with the maximum capacity of 2 MW in feeder 2. All feeders are determined to be AC. The total planning cost is \$11,117,190 with a cost breakdown of \$8,379,934 for the investment cost and \$2,737,252 for the operation cost. The total cost of supplying loads during the planning horizon without the microgrid deployment would be \$14,548,920 which shows that the installation of the microgrid is economically viable.

Case 1: The impact of changing the ratio of DC loads α on the type of the microgrid, the installation of DERs, and planning costs is studied in this case. The type

of feeders, i.e., either AC (associated with z=0) or DC (associated with z=1), the installed capacity of DERs, and the point of connection of the DES and renewable DGs to feeders are represented in Table 3.2. Table 3.3 summarizes the microgrid investment, operation, and planning costs for different values of α. For values of α between 0 and 0.6, all feeders would be AC. By increasing α to 0.7 and 0.8, feeders 1 and 2 are selected to be DC due to higher DC load compared to feeder 3. By increasing α to 0.9 and 1 (meaning that all the loads in the microgrid are DC), all feeders would be DC. For all values of α, the microgrid planning solution would install wind and solar units at their maximum capacity, conceivably due to their negligible operation costs. By increasing α from 0 to 0.7, the total installed capacity of dispatchable units increases, so the microgrid investment cost increases. The operation cost would increase as well since the hourly power generation of dispatchable units increases. Therefore, the planning cost would increase by increasing α from 0 to 0.7.

Table 3.2 Feeder Types and Installed DER Capacity (MW) with Respect to Ratio of DC Loads

Ratio of DC Load	Feeder Optimal Type			DERs										
				Installed Capacity of Dispatchable DGs				Wind		Solar		Storage		
								Feeder No.	Cap.	Feeder No.	Cap.	Feeder No.	P	E
	1	2	3	1	2	3	4							
0.0	AC	AC	AC	0.048	0.048	2.167	2.167	2	2.0	3	2.0	-	0	0
0.1				0.048	0.048	2.219	2.219	2	2.0	3	2.0	-	0	0
0.2				0.049	0.049	2.272	2.272	2	2.0	2	2.0	-	0	0
0.3				0.050	0.050	2.325	2.325	1	2.0	1	2.0	-	0	0
0.4				0.049	0.049	2.376	2.376	2	2.0	2	2.0	-	0	0
0.5				0.051	0.051	2.429	2.429	2	2.0	2	2.0	-	0	0
0.6				0.053	0.053	2.481	2.481	1	2.0	2	2.0	-	0	0

0.7	DC	DC	AC	0.055	0.055	2.534	2.534	3	2.0	1	2.0	-	0	0
0.8	DC	DC	AC	0	0	2.386	2.386	3	2.0	2	2.0	-	0	0
0.9	DC	DC	DC	0	0	2.122	2.122	3	2.0	3	2.0	3	0.15	0.76
1.0	DC	DC	DC	0	0	2.122	2.122	3	2.0	3	2.0	3	0.11	0.44

Table 3.3 Microgrid Costs with Respect to Ratio Of DC Loads

Ratio of DC Load	Investment Cost ($)	Operation Cost ($)	Planning Cost ($)	Total Cost without MG ($)
0.0	7,971,634	1,013,403	8,985,037	12,305,810
0.1	8,073,077	1,443,375	9,516,452	12,866,590
0.2	8,177,006	1,872,492	10,049,498	13,427,370
0.3	8,279,570	2,303,688	10,583,258	13,988,150
0.4	8,379,934	2,737,252	11,117,186	14,548,920
0.5	8,484,488	3,166,727	11,651,215	15,109,700
0.6	8,588,628	3,596,657	12,185,285	15,670,480
0.7	8,692,648	4,026,716	12,719,364	16,231,260
0.8	8,832,766	4,057,311	12,890,077	16,792,040
0.9	8,945,022	3,252,891	12,197,913	17,352,810
1.0	8,783,130	2,658,670	11,441,800	17,913,590

By increasing α to 0.9 or 1.0, the total installed capacity of dispatchable units decreases, and the DES would be installed since all feeders are DC. As a result of the DES installation, the total investment cost increases. However, the operation and planning costs would decrease. The investment cost slightly drops for α=1 since all loads in the microgrid are DC and the investment cost of inverters is eliminated. The operation cost drops since by selecting all feeders to be DC, the power loss in the converters will be reduced. Therefore, lower power generation of dispatchable DGs and lower imported power from the utility grid in different hours would be required.

The increase followed by the decrease in the microgrid investment and operation costs causes the microgrid planning cost to increase and then decrease, with the

maximum planning cost occurring at α=0.8. As a result, the threshold ratios of DC loads could be identified which make DC feeders economically more viable solutions than AC feeders. According to Table 3.2, for α=0.8 where both AC and DC feeders exist, the solar unit would be connected to a DC feeder, i.e., either 1 or 2, and the wind unit would be connected to feeder 3, which is AC, in order to eliminate the cost of voltage conversion.

According to Table 3.3, the microgrid planning cost is always lower than the total cost of supplying loads without microgrid installation, meaning that the microgrid is economically viable for all values of the DC loads. It should be also noted that the microgrid reliability cost would be zero for all values of α since the installed capacity of dispatchable units is adequate to fully supply the critical loads.

Case 2: The impact of changing the ratio of critical loads β on planning results is studied in this case. Results are provided in Tables 3.4 and 3.5. The microgrid planning solution would determine all feeders to be AC for different values of β. This result is expected since the ratio of DC loads does not change. According to Table 3.4, β has a significant effect on the installed capacity of dispatchable units. All DGs would be installed for different values of β, and renewable generation units are installed with full capacity. By increasing β, larger dispatchable capacity would be installed to supply all the critical loads, therefore the microgrid investment cost and the planning cost would increase. In this case, dispatchable units 3 and 4 are installed with higher capacity compared to units 1 and 2. The reason is that although units 3 and 4 have higher annualized investment costs compared to that of units 1 and 2, they offer a less expensive power generation, hence ensuring a reduced operation cost. According to Table 3.5, the

operation cost would decrease by increasing the ratio of critical loads. The reason is that increasing β would cause an increase in the total installed capacity of dispatchable units, while the total load has not changed. Therefore, there would be excess power generation in the microgrid which is sold to the utility grid. Selling power to the utility grid would increase the microgrid revenue thus decreasing the operation cost. Since there is not any change in the microgrid total load or converters' efficiencies, the cost of supplying loads without the microgrid deployment would remain unchanged, but still higher than the microgrid planning cost for all values of β.

Table 3.4 Feeder Types and Installed DER Capacity (MW) with Respect to Ratio of Critical Loads

Ratio of Critical Load	Feeder Optimal Type			DERs										
				Installed Capacity of Dispatchable DGs				Wind		Solar		Storage		
								Feeder #	Cap.	Feeder #	Cap.	Feeder #	P	E
	1	2	3	1	2	3	4							
0.0-0.5	AC	AC	AC	0.049	0.049	2.376	2.376	2	2.0	2	2.0	-	0	0
0.6				0.171	0.171	2.376	2.376	2	2.0	2	2.0	-	0	0
0.7				0.595	0.595	2.376	2.376	3	2.0	3	2.0	-	0	0
0.8				1.019	1.019	2.376	2.376	3	2.0	2	2.0	-	0	0
0.9				1.444	1.444	2.376	2.376	3	2.0	2	2.0	-	0	0
1.0				1.868	1.868	2.376	2.376	2	2.0	3	2.0	-	0	0

Table 3.5 Microgrid Costs with Respect to Ratio of Critical Loads

Ratio of Critical Load	Investment Cost ($)	Operation Cost ($)	Planning Cost ($)	Total Cost without MG ($)
0.0-0.5	8,379,934	2,737,252	11,117,186	14,548,920
0.6	8,493,422	2,648,368	11,141,790	
0.7	8,890,879	2,570,115	11,460,994	
0.8	9,288,336		11,858,451	

0.9	9,685,793		12,255,908	
1.0	10,083,250		12,653,365	

Case 3: The effect of inverters' and rectifiers' efficiencies η is studied in this case. Results are represented in Tables 3.6 and 3.7. Similar to previous cases, changing converters' efficiency while other parameters are kept constant, does not affect the type of feeders. Since there is less power loss by increasing converters' efficiencies, lower capacity of dispatchable DGs would be required to supply loads, hence the investment cost would decrease. On the other hand, since the hourly power generated by dispatchable DGs decreases following the increase in converters' efficiencies and also a lower amount of energy is imported from the utility grid due to lower power losses, the microgrid operation cost would decrease as well. Therefore, the installation of high-efficiency converters would decrease the microgrid planning cost. According to Table 3.7, since the microgrid planning cost is less than the cost of supplying loads without microgrid deployment, the microgrid installation would be economically viable for all values of η. The planning results also show that the microgrid reliability cost for all values of converters' efficiencies is zero.

Table 3.6 Feeder Types and Installed DER Capacity (MW) with Respect to Converters' Efficiency

Converters' Efficiency	Feeder Optimal Type			DERs										
				Installed Capacity of Dispatchable DGs				Wind		Solar		Storage		
								Feeder #	Cap.	Feeder #	Cap.	Feeder #	P	E
	1	2	3	1	2	3	4							
0.7	AC	AC	AC	0.049	0.049	2.376	2.376	2	2.0	2	2.0	-	0	0
0.8				0.016	0.016	2.235	2.235	1	2.0	2	2.0	-	0	0
0.9				0.007	0.007	2.115	2.115	1	2.0	2	2.0	-	0	0
0.95				0.053	0.053	2.069	2.069	3	2.0	3	2.0	-	0	0

Table 3.7 Microgrid Costs with Respect to Converters' Efficiency

Converters' Efficiency	Investment Cost ($)	Operation Cost ($)	Planning Cost ($)	Total Cost without MG ($)
0.7	8,379,934	2,737,252	11,117,190	14,548,920
0.8	8,164,430	1,657,549	9,821,979	13,669,940
0.9	7,998,331	730,559	8,728,889	12,986,280
0.95	7,980,876	270,535	8,251,411	12,698,430

Case 4: In this case, the effect of changing the electricity market price on the planning solution is studied. Results are shown in Tables 3.8 and 3.9. Based on the obtained results, changing the market price does not affect the type of feeders. In other words, all feeders would be AC, similar to the result obtained from the base case, since the ratio of DC loads remains unchanged. According to Table 3.8, by decreasing market prices in all hours by 10%, the microgrid planning solution would install dispatchable units 3 and 4 with lower capacities and also the solar unit with the maximum allowable capacity. The reason of reduction in the capacity of units 3 and 4 is that the decrease in market prices makes it economical to purchase more energy from the utility grid rather than relying on local generation. Therefore, the investment cost would decrease while the operation cost would increase. It should be also noted that the wind unit would not be economical to install in this case, but the solar unit is installed as its generation pattern coincides with market prices and load variations.

Table 3.8 Installed DER Capacity (MW) with Respect to Market Prices

Price Change Coefficient	DERs							
	Installed Capacity of Dispatchable DGs				Wind		Solar	
	1	2	3	4	Feeder #	Cap.	Feeder #	Cap.
-10%	0	0	2.122	2.122	-	0	3	2.0
Original Price	0.049	0.049	2.376	2.376	2	2.0	2	2.0
+10%	0.076	0.076	2.432	2.432	3	2.0	2	2.0

+20%	0.085	0.085	2.530	2.530	3	2.0	2	2.0
+30%	0.056	0.056	2.606	2.606	3	2.0	2	2.0

Table 3.9 Microgrid Costs with Respect to Market Prices

Price Change Coefficient	Investment Cost ($)	Operation Cost ($)	Planning Cost ($)	Total Cost without MG ($)
-10%	5,528,558	6,427,358	11,955,916	13,107,390
Original Price	8,379,934	2,737,252	11,117,186	14,548,920
+10%	8,478,715	1,537,441	10,016,156	15,990,460
+20%	8,614,995	216,965	8,831,960	17,432,000
+30%	8,686,841	-1,076,090	7,610,751	18,873,540

By increasing the market price, it would be more desirable for the microgrid to sell energy to the utility grid, meaning that power exchange would be negative in many hours which reduces the operation cost. As a result, a larger dispatchable capacity should be installed, which causes the investment cost to increase. By increasing market prices by 30%, the microgrid would sell as much energy as possible to the utility grid such that the operation cost becomes negative, meaning that the microgrid has revenue from energy exchange with the utility grid.

According to Table 3.9, the microgrid total planning cost decreases by increasing market prices, while the total cost of supplying loads without the microgrid deployment increases, meaning that the microgrid deployment would be an economical solution when market prices increase. It should be finally noted that similar to previous cases, all critical loads would be supplied for all values of market prices, so the reliability cost is zero.

3.4 Discussions

The proposed hybrid microgrid planning model offers various features and provides an insight on the microgrid planning decisions:

- Ratio of DC loads: The most decisive factor in determining the type of each feeder within the microgrid distribution network is the ratio of DC loads in each feeder. By increasing this parameter, more feeders are selected to be DC. Since changing this ratio would alter the total cost, it can be used as a tool to determine the turning point for the type of feeders from AC to DC or DC to AC.
- Removing the cost of power conversion: In cases with both AC and DC feeders in the microgrid, the wind turbine is installed in AC feeders and the solar PV and DES are installed in DC feeders to avoid the cost of power conversion.
- Tradeoff between operation and investment costs: Among AC dispatchable units, those offering a less expensive power would be installed with larger capacities although their capital costs might be higher. Moreover, the wind and solar units would be installed with maximum capacity in almost all cases because their operation cost is zero.
- Changes in the operation cost: Increasing critical loads, converters' efficiencies, or market prices would cause a decrease in the operation cost. Specifically for critical loads, by increasing their percentage a larger dispatchable capacity would be installed. Since the total load in the microgrid does not change, there is excess generated power which would be sold to the utility grid. Therefore, the operation cost would decrease.
- Importance of more efficient converters: By using highly efficient converters, there would be less power loss in the microgrid. Therefore, not only are dispatchable

units installed with lower capacities, which reduce the investment cost, but also less energy would be imported from the utility grid, which reduces the operation cost.

- Impact of market prices: By increasing market prices, it would be desirable for the microgrid to install a larger dispatchable capacity in order to sell as much energy as possible to the utility grid, which increases the microgrid revenue by decreasing the operation cost.
- The microgrid economic viability: The proposed model is also capable of ensuring the microgrid economic viability. According to the obtained results in all studied cases, the microgrid deployment is economically viable since the planning cost is lower than the total cost of supplying loads without the microgrid deployment.

4. Chapter Four: Co-Optimization Generation and Distribution Planning in Microgrids

This chapter presents a co-optimization generation and distribution planning in microgrids which aims at minimizing the microgrid long-term operation cost while ensuring a reliable supply of loads. One solution to increase the distribution network reliability and prevent load curtailment is to build new distribution lines or to reinforce the existing lines through upgrades. Another solution is to install DERs in strategic locations in distribution network. In this study, both these solutions are considered simultaneously, allowing the identification of the most viable solution. Various types of DERs are considered in this study in which their optimal size and location are determined through the proposed model. The power flow equations are linearized, using minor approximations, in order to be able to formulate the problem using MILP.

One important issue in managing microgrids is the role of uncertainties. Uncertainty represents factors, which having a major influence on scheduling decisions, are out of control of the microgrid controller and/or cannot be forecasted with certainty. Uncertainty considerations in power system operation and planning have been significantly increased in the past few years. Two common approaches for considering uncertainty are stochastic programming and robust optimization. Stochastic models are commonly based on sampling methods with pre-assumed probability distribution functions, which convert the original objective to the weighted average of objectives for

individual scenarios. However, a concrete characterization of the uncertainty requires a large number of scenarios, especially when uncertainties are not discrete. Thus, the derived large-scale stochastic problem is more time-intensive and considerably harder to solve than the original problem. In addition, probability distributions cannot be accurately estimated which would obstruct the practical implementation of this technique. On the other hand, in robust optimization, each uncertain parameter is associated with an uncertainty interval, i.e., an upper bound and a lower bound, where the optimization problem ensures the feasibility of the solution in the worst-case scenarios [17]. Thus, in contrast with stochastic programming, there is no need to accurately determine distribution probability functions related to uncertain data. Furthermore, the robust optimization problem does not suffer from the curse of dimensionality since only one robust problem is solved rather than a set of problems corresponding to individual scenarios. However, the robust optimization solution is obtained at the expense of sacrificing a certain level of the solution optimality and increased computational complexity. This chapter further proposes a preprocess approach to identify uncertainties that result in the robust (i.e., worst-case) solution [58]. In other words, the solution of the robust optimization will be achieved without the need to solve the robust problem. Using this preprocess approach, the primal microgrid operation problem, which is linear and convex, can be solved instead of the dual problem that is required in the robust optimization and contains a large number of binary variables, hence addressing the computational complexity problem. This study performs studies on the microgrid optimal scheduling problem which also acts as a core component in longer term maintenance and planning problems.

4.1 Model Outline and Formulation of Co-Optimization Generation and Distribution Planning in Microgrids

There are both dispatchable and nondispatchable candidate DGs in a microgrid. Nondispatchable DGs are renewable energy sources such as solar PV and wind. Distributed energy storage (DES) is employed in order to increase the controllability and dispatchability of these energy sources. DES is charged at off-peak hours with low electricity prices and discharged at peak hours when electricity price is high. The microgrid is connected to the utility grid to exchange power as needed and further govern voltage and frequency. One significant feature of the microgrid is its islanding capability which allows operation in the islanded mode in case of any disturbance in the upstream grid. Islanding is defined as a set of scenarios in the planning problem as will be further explained. The microgrid can buy power from the utility grid, associated with positive exchanged power, or sell back the excess power to the utility grid, associated with negative exchanged power which increases the microgrid revenue. A number of candidate distribution lines between predetermined buses are considered in order to alleviate potential congestion in existing lines. The solution of the optimization problem determines the optimal size and location of DERs as well as the installation of lines.

The proposed co-optimization generation and distribution planning problem aims at minimizing the microgrid total planning cost (4.1) comprising of the investment cost of DERs and distribution lines (*IC*), the operation cost (*OC*), and the reliability cost (*RC*), similar to what was discussed in Chapters two and three. It should be noted that the investment cost is calculated annually while the operation and reliability costs are

calculated hourly for all hours and days in the planning horizon. The investment, operation, and reliability costs are defined in (4.2)-(4.4), respectively.

$$\min \sum_{t} \kappa_t \left(IC_t + OC_t + RC_t \right) \tag{4.1}$$

$$IC_t = \sum_{i \in \{\mathrm{G,W}\}} CC_{it} P_i^{\max} + \sum_{i \in \mathrm{E}} \left(CP_{it} P_i^{\max} + CE_{it} C_i^{\max} \right) + \sum_{l \in \mathrm{L}} CL_{lt} o_l \qquad \forall t \tag{4.2}$$

$$OC_t = \sum_{h} \sum_{b} \sum_{i \in \mathrm{G}} c_i P_{ibht0} + \sum_{h} \sum_{b} \rho_{bht} P_{M,bht0} \qquad \forall t \tag{4.3}$$

$$RC_t = \sum_{s} pr_s \sum_{h} \sum_{b} \sum_{\mathrm{m}} vLS_{mbhts} \qquad \forall t \tag{4.4}$$

The investment cost (4.2) comprises the investment cost of dispatchable and nondispatchable DGs (derived by multiplying the DGs' annualized capital cost by their installed capacity), investment cost of the DES, and investment cost of distribution lines. The DES investment cost has two components associated with installed power capacity and energy capacity, in which both are calculated as the associated annualized capital cost times installed capacity. The investment cost of line is determined as the given annualized capital cost times a binary investment variable, o_l. The binary variable is employed to consider the installation of distribution lines; that is if a candidate line is installed, o_l would be one, otherwise it is zero. The operation cost (4.3) consists of two terms, the operation cost of dispatchable DGs calculated by their generation price times generated power in each hour, and cost of power exchanged with the utility grid, calculated by electricity market price times the amount of exchanged power with the utility grid. Both terms are aggregated over all hours and days in the planning horizon. The reliability cost (4.4) represents the cost of unserved energy and is defined as the value of lost load (VOLL) times the amount of hourly load curtailment, aggregated over

all hours, days, and islanding scenarios in the planning horizon. A comprehensive discussion on VOLL for different types of customers can be found in [59]. The operation and reliability costs are further summed over the considered scenarios (for grid-connected and islanded operation) based on the associated probability. In (4.3), s=0 represents the grid-connected mode. The objective function (4.1) is further subject to DERs and power balance constraints (4.5)-(4.19) and power flow equations (4.20)-(4.28) [60].

DERs and Power Balance Constraints: A binary decision variable, x_{im}, is used to determine the location of DER installations, which would be one when DER i is installed at bus m, and zero otherwise. Constraint (4.5) ensures that each DER is connected to only one bus. The total dispatchable capacity should be larger than the microgrid critical load to ensure a reliable supply of loads when operating in the islanded mode (4.6). The active load balance equation (4.7) ensures that the generated power from all DERs and lines connected to each bus plus the exchanged power with the utility grid at the point of interconnection (POI) is equal to the hourly load demand minus the amount of curtailed load. Similarly, the reactive load balance equation (4.8) ensures that the reactive power from all DERs and lines connected to each bus plus the exchanged reactive power with the utility grid is equal to the amount of hourly reactive load. The exchanged power with the utility grid is limited by the capacity of the line connecting the microgrid to the utility grid (4.9). The amount of hourly generated power of dispatchable DGs cannot exceed their installed capacity (4.10). The hourly power generated by nondispatchable DGs is determined by a normalized forecasted generation times the associated installed capacity (4.11). Additionally, installed DG capacity

cannot exceed its allowable installation capacity limits (4.12), which is determined based on budget or space limitations. The load curtailment at each bus cannot exceed its hourly load demand (4.13). The DES constraints are represented in (4.14)-(4.19). The DES power in both discharging and charging modes is limited by its installed power capacity (4.14)-(4.15). The DES stored energy is determined based on the net charged power, efficiency, and the stored energy in previous hours (4.16). Additionally, the DES net charge is assumed to be zero at the end of each day in the planning horizon (4.17). Finally, the installed DES power and energy capacity are limited by its allowable power and energy capacity limits, respectively (4.18)-(4.19).

$$\sum_{m} x_{im} \le 1 \qquad \forall i \in \{\mathrm{G}, \mathrm{W}, \mathrm{E}\} \tag{4.5}$$

$$\beta \sum_{m} PD_{mbht}^{\max} \le \sum_{i \in \mathrm{G}} P_i^{\max} \tag{4.6}$$

$$\sum_{i \in \{\mathrm{G},\mathrm{W}\}} P_{ibhts} x_{im} + \sum_{i \in \mathrm{E}} \left(P_{ibhts}^{dch} - P_{ibhts}^{ch} \right) x_{im} + \sum_{l \in \mathrm{L}_m} PL_{lbhts} + P_{M,mbhts} = PD_{mbht} - LS_{mbht} \tag{4.7}$$
$$\forall m, \forall b, \forall h, \forall t, \forall s$$

$$\sum_{i \in \{\mathrm{G},\mathrm{W}\}} Q_{ibhts} x_{im} + \sum_{l \in \mathrm{L}_m} QL_{lbhts} + Q_{M,mbhts} = QD_{mbht} \qquad \forall m, \forall b, \forall h, \forall t, \forall s \tag{4.8}$$

$$-P_M^{\max} u_{M,bhts} \le P_{M,bhts} \le P_M^{\max} u_{M,bhts} \qquad \forall b, \forall h, \forall t, \forall s \tag{4.9}$$

$$0 \le P_{ibhts} \le P_i^{\max} \qquad \forall i \in \mathrm{G}, \forall b, \forall h, \forall t, \forall s \tag{4.10}$$

$$P_{ibhts} = P_i^{\max} \zeta_{ibht} \qquad \forall i \in \mathrm{W}, \forall b, \forall h, \forall t, \forall s \tag{4.11}$$

$$P_i^{\max} \le P_i^{cap} \sum_{m} x_{im} \qquad \forall i \in \{\mathrm{G}, \mathrm{W}\} \tag{4.12}$$

$$LS_{mbhts} \le PD_{mbhts} \qquad \forall m, \forall b, \forall h, \forall t, \forall s \tag{4.13}$$

$$0 \le P_{ibhts}^{dch} \le P_i^{\max} \qquad \forall i \in \mathrm{E}, \forall b, \forall h, \forall t, \forall s \tag{4.14}$$

$$0 \le P_{ibhts}^{ch} \le P_i^{\max} \qquad \forall i \in \mathrm{E}, \forall b, \forall h, \forall t, \forall s \tag{4.15}$$

$$0 \le \sum_{k \le b} (P_{ikhts}^{ch} - P_{ikhts}^{dch} / \eta_i) \le C_i^{\max} \quad \forall i \in \mathrm{E}, \forall b, \forall h, \forall t, \forall s \tag{4.16}$$

$$\sum_{b} (P_{ibhts}^{ch} - P_{ibhts}^{dch} / \eta_i) = 0 \qquad \forall i \in \mathrm{E}, \forall h, \forall t, \forall s \tag{4.17}$$

$$P_i^{\max} \le P_i^{cap} \sum_m x_{im} \qquad \forall i \in \mathrm{E} \tag{4.18}$$

$$C_i^{\max} \le C_i^{cap} \sum_m x_{im} \qquad \forall i \in \mathrm{E} \tag{4.19}$$

Power Flow Constraints: Power flow equations are nonlinear and cannot be directly included in the developed MILP formulation. Assumptions (4.20) and (4.21) are applied to linearize the equations. Voltage magnitudes and angles are considered as those of bus 1 (i.e., the POI) plus deviations, as represented in (4.22) and (4.23). The resulting multiplication of voltage magnitude and voltage angle variables is very small and thus can be eliminated from power flow equations.

$$\sin(\theta_{mbhts} - \theta_{nbhts}) \approx \theta_{mbhts} - \theta_{nbhts} \quad \forall mn \in \mathrm{L}, \forall b, \forall h, \forall t, \forall s \tag{4.20}$$

$$\cos(\theta_{mbhts} - \theta_{nbhts}) \approx 1 \qquad \forall mn \in \mathrm{L}, \forall b, \forall h, \forall t, \forall s \tag{4.21}$$

$$V_{mbhts} = 1.0 + \Delta V_{mbhts} \qquad \forall m, \forall b, \forall h, \forall t, \forall s \tag{4.22}$$

$$\theta_{mbhts} = 0 + \Delta\theta_{mbhts} \qquad \forall m, \forall b, \forall h, \forall t, \forall s \tag{4.23}$$

The linear active and reactive power flow equations for distribution lines are represented by (4.24) and (4.25), respectively. If a candidate line is not installed, o_l would be zero, and (4.24)-(4.25) would be relaxed. Therefore, the real and reactive

powers passing through the lines would be zero according to (4.26) and (4.27). Likewise, if the solution of the optimization problem is to install a line, o_l would be one, and real and reactive powers would be respectively determined by (4.24) and (4.25) with the limits imposed by (4.26) and (4.27). It should be noted that (4.24) and (4.25) are nonlinear and are solved in a two-stage fashion. The term $\sum_{m\in B_l} a_{lm} \triangle V_{mbhts}$ is considered zero in stage one, and then by finding $\triangle V_{mbhts}$, this term will be replaced, and the problem is solved again in stage two. Finally, the voltage magnitudes at all buses cannot exceed their minimum and maximum limits (4.28).

$$\begin{aligned} &-M(1-o_l) \le PL_{lbhts} - g_l(1+\sum_{m\in B_l} a_{lm1}\Delta V_{mbhts})\sum_{m\in B_l}\left((a_{lm2}-a_{lm1})\Delta V_{mbhts}\right) \\ &+b_l\sum_{m\in B_l}(a_{lm2}-a_{lm1})\Delta\theta_{mbhts} \le M(1-o_l) \qquad \forall l,\forall b,\forall h,\forall t,\forall s \end{aligned} \tag{4.24}$$

$$\begin{aligned} &-M(1-o_l) \le QL_{lbhts} + b_l(1+\sum_{m\in B_l} a_{lm1}\Delta V_{mbhts})\sum_{m\in B_l}\left((a_{lm2}-a_{lm1})\Delta V_{mbhts}\right) \\ &+g_l\sum_{m\in B_l}(a_{lm2}-a_{lm1})\Delta\theta_{mbhts} \le M(1-o_l) \qquad \forall l,\forall b,\forall h,\forall t,\forall s \end{aligned} \tag{4.25}$$

$$-PL_l^{\max} o_l \le PL_{lbhts} \le PL_l^{\max} o_l \qquad \forall l,\forall b,\forall h,\forall t,\forall s \tag{4.26}$$

$$-QL_l^{\max} o_l \le QL_{lbhts} \le QL_l^{\max} o_l \qquad \forall l,\forall b,\forall h,\forall t,\forall s \tag{4.27}$$

$$\Delta V_m^{\min} \le \Delta V_{mbhts} \le \Delta V_m^{\max} \qquad \forall m,\forall b,\forall h,\forall t,\forall s \tag{4.28}$$

4.2 Model Outline and Formulation of Microgrid Optimal Scheduling Under Uncertainties

Uncertainties involved in the microgrid optimal scheduling can be attributed into two groups of forecasting-related and islanding-related. Forecast errors represent uncertainties in accurately forecasting future values of microgrid load, variable

renewable generation, and time-dependent market prices. The islanding-related uncertainty represents the uncertain time and duration of main grid outages in which the microgrid needs to operate in the islanded mode. An extensive discussion on uncertainties in microgrids can be found in [17]. This study only focuses on the forecasting-related uncertainty.

The day-ahead microgrid optimal scheduling problem is formulated as follows.

$$\max_{\mathrm{U}} \min_{\mathrm{P}} \sum_{b} \sum_{i \in \mathrm{G}} c_i P_{ib} + \sum_{b} \rho_b P_{M,b} + \sum_{b} v_b LS_b \tag{4.29}$$

$$\sum_{i \in \{\mathrm{G,W}\}} P_{ib} + \sum_{i \in \mathrm{E}} (P_{ib}^{dch} - P_{ib}^{ch}) + P_{M,b} + LS_b = PD_b \quad \forall b \tag{4.30}$$

$$-P_M^{\max} u_{M,b} \le P_{M,b} \le P_M^{\max} u_{M,b} \qquad \forall b \tag{4.31}$$

$$0 \le P_{ib} \le P_i^{\max} \qquad \forall i \in \mathrm{G}, \forall b \tag{4.32}$$

$$P_{ib} = \hat{P}_{ib} \qquad \forall i \in \mathrm{W}, \forall b \tag{4.33}$$

$$0 \le P_{ib}^{dch} \le P_i^{\max} \qquad \forall i \in \mathrm{E}, \forall b \tag{4.34}$$

$$0 \le P_{ib}^{ch} \le P_i^{\max} \qquad \forall i \in \mathrm{E}, \forall b \tag{4.35}$$

$$0 \le \sum_{\tau \le b} (P_{ib}^{ch} - P_{ib}^{dch} / \eta_i) \le C_i^{\max} \qquad \forall i \in \mathrm{E}, \forall b \tag{4.36}$$

$$0 \le LS_b \le PD_b \qquad \forall b \tag{4.37}$$

The objective of the optimal scheduling problem is to minimize the microgrid operation cost (4.29), including the generation cost of dispatchable units, the cost of energy purchase from the main grid, and the cost of unserved energy. The objective is maximized over uncertainty sets to achieve the worst-case microgrid optimal operation solution. The load balance equation (4.30) ensures that the sum of power generated by

all DERs, including dispatchable and nondispatchable units as well as DES, and power from the main grid is equal to the hourly load. Additional operational constraints include the limit the amount of exchanged power with the main grid (4.31), dispatchable units' generation capacity limits (4.32), nondispatchable units generation (4.33), the DES charging and discharging limits (4.34)-(4.35), the DES available energy (4.36), and the limit on load curtailments (4.37). A binary islanding parameter is added to (4.31) to model grid-connected ($u_{M,b}$=1) and islanded ($u_{M,b}$=0) operation modes. Since line flows are relatively small, the distribution network congestion is neglected. The proposed microgrid optimal scheduling model is developed in a linear format where the binary variables associated with the commitment state of dispatchable units and charging/discharging states of DES are ignored.

To solve the proposed microgrid optimal scheduling problem, in which its objective has a max-min format, the dual problem of the inner minimization problem is combined with the outer maximization problem. The resultant problem with dual variables and uncertain parameters is as follows:

$$\max_{\mathrm{U,D}} \sum_b \lambda_b \hat{D}_b + \sum_b (\mu_b^- + \mu_b^+) P_M^{\max} u_{M,b} + \sum_b \sum_{i\in \mathrm{W}} \vartheta_{ib} \hat{P}_{ib} + \sum_b \sum_{i\in \mathrm{G}} \pi_{ib} P_i^{\max} + \sum_b \sum_{i\in \mathrm{E}} \psi_{ib}^{dch} P_i^{\max} + \sum_b \sum_{i\in \mathrm{E}} \psi_{ib}^{ch} P_i^{\max} + \sum_b \sum_{i\in \mathrm{E}} \xi_{ib}^{+} C_i^{\max} + \sum_b \sigma_b P\hat{D}_b \tag{4.38}$$

$$\lambda_b + \pi_{ib} \le c_i \qquad \forall i \in \mathrm{G}, \forall b \tag{4.39}$$

$$\lambda_b + \vartheta_{ib} = 0 \qquad \forall i \in \mathrm{W}, \forall b \tag{4.40}$$

$$\lambda_b + \psi_{ib}^{dch} - \sum_{\tau \ge b} (\xi_{i\tau}^{+} - \xi_{i\tau}^{-}) / \eta_i \le 0 \qquad \forall i \in \mathrm{E}, \forall b \tag{4.41}$$

$$-\lambda_b + \psi_{ib}^{ch} + \sum_{\tau \ge b} (\xi_{i\tau}^{+} - \xi_{i\tau}^{-}) \le 0 \qquad \forall i \in \mathrm{E}, \forall b \tag{4.42}$$

$$\lambda_b + (\mu_b^+ - \mu_b^-) = \rho_b \qquad \forall b \qquad (4.43)$$

$$\lambda_b + \sigma_b \leq v_b \qquad \forall b \qquad (4.44)$$

where λ, μ, π, υ, ψ^{dch}, ψ^{ch}, ξ, and σ are dual variables of constraints (4.30)-(4.37), respectively. Considering polyhedral uncertainty sets, and assuming that the worst-case solution occurs at extreme points, uncertain parameters can be represented as a function of the nominal forecasted value and the uncertainty interval with the aid of auxiliary binary variables. For example, the uncertain parameter y can be written as $y = \tilde{y}_b - \underline{y}_b \underline{u}_b + \overline{y}_b \overline{u}_b$ where inserted bars represent its upper/lower bounds. To prevent simultaneous occurrence of extreme points, one binary variable can be set at one at any given hour, i.e., $\underline{u}_b + \overline{u}_b \leq 1$. Compared to the primal problem which was a linear problem, a large amount of binary variables will be added to the robust problem. The addition of binary variables would create a nonlinear and computationally more challenging optimization problem. Bilinear terms, as would appear in (4.38) when binary variables are used, should be further converted into linear terms which would accordingly add additional variables to the problem [61].

4.2.1 Uncertainty Control

The level of solution conservatism can be efficiently controlled by limiting the total number of uncertain parameters that can reach their extreme values, or in other words, the total number of binary auxiliary variables that can reach a value of 1. The limit on uncertainty options is given in (4.45). The larger the limit on uncertainty option, a more robust solution is obtained against uncertainties, resulting in a larger operation cost. On the other hand, the smaller the limit on uncertainty option, a more aggressive

solution is obtained, resulting in a less robust solution. A moderate solution considers some level of uncertainty in between.

$$\sum_{b}(\underline{u}_b + \overline{u}_b) \le \Gamma_b \qquad \forall b \qquad (4.45)$$

The limit on uncertainty option is a necessary tool to control the solution conservatism and prevent large deviations from the optimal solution. This limit, however, adds additional computational complexity to the problem as only a selected set of binary variables can reach a value of 1. To address the computational complexity, a preprocessing approach, as discussed in the next Section, is proposed.

4.3 Proposed Preprocessing Approach

The objective of the proposed preprocessing approach is to determine uncertainties without the need to solve the computationally challenging robust optimization problem developed in Section 4.2. To perform preprocessing, first a set of efficient signals for each type of uncertainty should be developed as discussed in the following:

Load signal: Considering the proposed uncertainty definition, the load uncertainty will be defined as $PD = \widetilde{PD}_b - \underline{PD}_b \underline{u}_b^l + \overline{PD}_b \overline{u}_b^l$ and the corresponding term in the objective function (10) would be $\sum_b (\lambda_b + \sigma_b)(\widetilde{PD}_b - \underline{PD}_b \underline{u}_b^l + \overline{PD}_b \overline{u}_b^l)$. It can be shown that λ_t, i.e., the dual variable associated with the load balance constraint (4.30), is always positive in the proposed robust problem, and also θ_b is zero in grid-connected modes as there will be no load curtailments. Therefore, demand will maximize the objective (4.38) when it is larger than the forecasted value, or equivalently, when it is at its upper bound, i.e., $\overline{u}_b^l = 1$ and $\underline{u}_b^l = 0$. The uncertain load

will be accordingly represented by $\widetilde{PD}_b + \overline{PD}_b$. Considering that the upper and lower bounds of the uncertainty interval are linear functions of the nominal value, e.g., $\overline{PD}_b = 0.1 \times \widetilde{PD}_b$ for a 10% forecast error, the load signal of $\lambda_b(\widetilde{PD}_b + \overline{PD}_b)$ will be considered for characterizing the load uncertainty. By calculating this signal and sorting values from the highest to the lowest, the order of hours of the day in which the worst-case load has happened can be efficiently determined.

Renewable generation signal: The renewable uncertainty will be defined as $P_{ib} = \tilde{P}_{ib} - \underline{P}_{ib}\underline{u}_{ib}^{g} + \overline{P}_{ib}\overline{u}_{ib}^{g}$. It can be shown that ϑ_{ib}, i.e., the dual variable associated with the generation of renewable sources (4.33), is always negative in the proposed robust problem. Therefore, variable renewable sources will maximize the objective (4.38) when they generate less than the forecasted value, or equivalently, when reaching the lower bound, i.e., $\underline{u}_{ib}^{g} = 1$ and $\overline{u}_{ib}^{g} = 0$. The power generated by variable renewable sources will be accordingly represented by $\tilde{P}_{ib} - \underline{P}_{ib}$. A lower value for $\vartheta_{ib}(\tilde{P}_{ib} - \underline{P}_{ib})$ will result in a larger impact on the objective value, hence this term will be considered as the signal to determine the worst-case scenario of uncertainties in renewable generation. By calculating this signal and sorting values from the lowest to the highest, the order of hours of the day in which the worst-case has happened would be determined.

Market price signal: The worst-case scenario of uncertainties in market prices depends on the microgrid power exchange with the main grid, i.e., selling or buying. If the microgrid is selling power in a specific hour, i.e., negative exchange power with the main grid, the worst-case in that hour would occur at the lower bound in which the market price is less than the forecasted value. Similarly, if the microgrid is buying power

in a specific hour, i.e., a positive exchange power with the main grid, the worst-case in that hour would occur at the upper bound in which the market price is more than the forecasted value. By changing market prices, generation prices of dispatchable units should be noted. If the market price in a specific hour is less than the generation price of a dispatchable unit, the microgrid would prefer to buy power from the main grid instead of dispatching that unit, therefore $P_{M,b}$ would be positive. The worst-case in this situation would occur when the market price is increased. If the market price in that hour increases to the extent that it becomes higher than the generation price of the dispatchable unit, the microgrid would prefer to dispatch that unit and sell power to the main grid. On the other hand, if the market price in a specific hour is higher than the generation price of a dispatchable unit, the microgrid would prefer to dispatch that unit and sell power to the main grid, therefore $P_{M,t}$ would be negative. The worst-case in this situation would occur when the market price is further decreased. As a result, the signal for measuring the uncertainty in market price would comprise two parts; one is the effect of the exchange power and change in the market price, and the other is the effect of changes in the market price on turning dispatchable units on or off. In summary and based on the discussions, $\Delta\rho_b . P_{M,b} + \Delta P_{ib} . (c_i - \rho_b - \Delta\rho_b)$ could be considered as a signal to determine the worst-case scenario of uncertainties in market prices. Again, by calculating the proposed signal and sorting values from the highest to the lowest, the order of hours of the day in which the worst-case has happened would be determined.

4.4 Numerical Simulations

4.4.1 Co-Optimization Generation and Distribution Planning

The IEEE standard 33-bus test system, as shown in Fig. 4.1 is used for microgrid installation. This system comprises 33 buses, 32 distribution lines, and 32 loads, with a maximum initial aggregated load of 2.7 MW [57]. Tables 4.1, 4.2, and 4.3 show the characteristics of candidate DGs, DES, and distribution lines, respectively. As renewable DGs have a negligible operation cost, their cost coefficient is assumed to be zero. The investment cost of the candidate lines is calculated based on studies in [62]. The hourly load demand, renewable generation, and market price data are forecasted based on the historical data from a practical system [63]. The DES efficiency is assumed to be 95%. The planning horizon is 20 years. No islanding scenarios are considered in simulations, meaning that the microgrid operates in grid-connected mode at all times. However, the proposed model can efficiently consider islanded operation. The microgrid planning problem is implemented on a high-performance computing server consisting of four 10-core Intel Xeon E7-4870 2.4 GHz processors. The problem is formulated by MILP and solved by CPLEX 12.6 [56], with average running time of 70 minutes. Following cases are studied.

Case 0: Base case microgrid planning

Case 1: Sensitivity analysis on the ratio of critical loads

Case 2: Sensitivity analysis on load demand

Case 3: Sensitivity analysis on market prices

Case 0: The ratio of critical loads to total load is considered to be 40% for all operation hours. It is assumed that DGs 1-6 can be installed in buses 17, 21, 32, 24, 15,

and 15, respectively, as end lines have lower capacity and congestion is more likely. It is further assumed that the DES can be installed in bus 15. The microgrid planning solution would install dispatchable DGs 3 (with 0.65 MW capacity) and 4 (with 0.44 MW capacity) as well as the solar unit (with 0.48 MW capacity). No candidate lines are installed in the base case. The total planning cost is $9,462,578 with a cost breakdown of $1,310,805 for the investment cost and $8,151,773 for the operation cost.

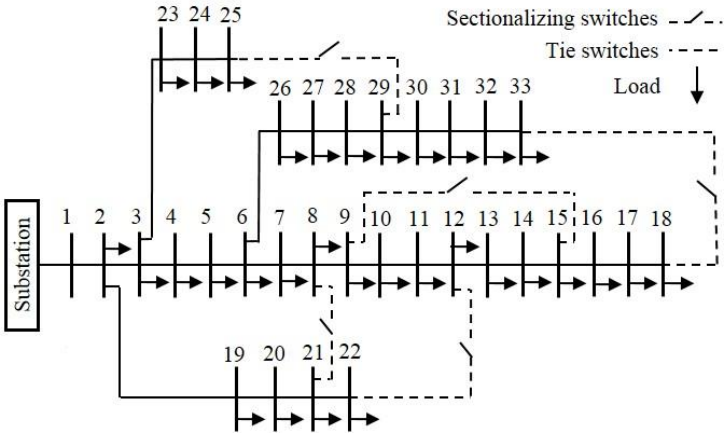

Fig. 4.1 IEEE 33-bus test system.

Table 4.1 Candidate DGs Characteristics

Unit Number	Type	Allowable installation capacity (MW)	Cost Coefficient ($/MWh)	Annualized Investment Cost ($/MW)
1	Gas	3	90	50,000
2	Gas	3	90	50,000
3	Gas	1	70	70,000
4	Gas	1	70	70,000
5	Wind	2	0	132,000
6	Solar	2	0	133,000

Table 4.2 Candidate DES Characteristics

Allowable Installation Capacity (MW)	Allowable Installation Energy (MWh)	Annualized Investment Cost – Power ($/MW)	Annualized Investment Cost – Energy ($/MWh)
1	6	60,000	30,000

Table 4.3 Candidate Lines Characteristics

Line	From bus	To bus	R(Ω)	X(Ω)	Line Capacity (kW)	Annualized Investment Cost ($)
33	12	13	1.468	1.155	500	37749
34	13	14	0.5416	0.7129	450	12534
35	14	15	0.591	0.526	300	9118
36	15	16	0.7463	0.545	250	9595
37	16	17	1.289	1.721	250	16573
38	17	18	0.732	0.574	100	3765
39	20	21	0.4095	0.4784	210	4423
40	21	22	0.7089	0.9373	110	4010
41	23	24	0.898	0.7091	1050	48492
42	24	25	0.896	0.7011	500	23040
43	30	31	0.9744	0.963	500	25056

Case 1: The impact of changing the ratio of critical loads, β, on planning results is studied in this case. The microgrid planning is studied two scenarios, with and without allowing installation of candidate lines, and results are tabulated in Table 4.4. The total dispatchable capacity increases by increasing the ratio of critical loads as the microgrid should be able to seamlessly supply critical loads. Therefore, the microgrid investment cost increases too by increasing β, as shown in Table V. By increasing the ratio of critical loads from 0 to 60%, none of the candidate lines are installed, but by increasing β to 0.8 and 1 (meaning all loads are considered as critical), lines 34, 35, and 39 are installed. The investment cost suddenly increases in comparison with the case without line installation. If there is no critical load in the microgrid (associated with β=0), only the solar unit is installed, but none of the dispatchable units, meaning that importing power from the utility grid is more economical than installing local DGs. It is worth mentioning that for the ratio of critical loads at 80% and 100%, a larger capacity of solar unit is also installed when the line installation is considered (increased from 0.48 MW to 0.78MW). The reason is that the solar unit is installed in bus 15, and lines 34 and 35 are respectively between buses 13-14 and 14-15, thus can help with transferring the additional generated

power. As total load does not change, there would be excess power to sell back to the utility grid, which causes the operation cost to decrease. As the increase in the investment cost is higher than the decrease in the operation cost, the planning cost would increase by increasing the ratio of critical loads. According to results, the planning cost would decrease in case of the installation of candidate lines, which means the simultaneous installation of DERs and distribution lines would be more economical. It should be noted that DES is not installed for any ratio of critical loads.

Table 4.4 Investment Plan with Respect to Changes in Ratio of Critical Loads

Ratio of Critical Load		1	2	3	4	5	6	Installed Lines
0	w/o lines	0	0	0	0	0	0.48	-
	w/ lines	0	0	0	0	0	0.48	-
0.2	w/o lines	0	0	0	0.55	0	0.48	-
	w/ lines	0	0	0	0.55	0	0.48	-
0.4	w/o lines	0	0	0.10	1.00	0	0.48	-
	w/ lines	0	0	0.10	1.00	0	0.48	-
0.6	w/o lines	0	0	0.65	1.00	0	0.48	-
	w/ lines	0	0	0.65	1.00	0	0.48	-
0.8	w/o lines	0.17	0.35	0.68	1.00	0	0.48	-
	w/ lines	0.17	0.35	0.66	1.00	0	0.78	34,35,39
1.0	w/o lines	0.28	0.76	0.68	1.00	0	0.48	-
	w/ lines	0.50	0.55	0.68	1.00	0	0.78	34,35,39

Table 4.5 Microgrid Costs with Respect to Ratio of Critical Loads

Ratio of Critical Load		Investment Cost ($)	Operation Cost ($)	Planning Cost ($)
0	w/o lines	596,650	8,809,487	9,406,137
	w/ lines			
0.2	w/o lines	953,736	8,459,261	9,412,997
	w/ lines			
0.4	w/o lines	1,310,805	8,151,77	9,462,578
	w/ lines			
0.6	w/o lines	1,668,653	7,864,340	9,532,993
	w/ lines			
0.8	w/o lines	1,932,385	7,759,704	9,692,089
	w/ lines	2,354,132	7,116,085	9,470,217
1.0	w/o lines	2,187,500	7,758,661	9,946,161

	w/ lines	2,613,157	7,082,358	9,695,515

Case 2: In this case, a sensitivity analysis of planning results with respect to the load demand is carried out. The installed DER capacity and installed lines are represented in Table 4.6. The hourly load in all years is increased by up to 100%, investigating additional cases with different load growth rates. As expected, by increasing the load demand, more DER capacity should be installed, which causes the investment cost to increase (Table 4.7). It should be noted that among dispatchable DGs, units 3 and 4, despite their higher capital costs, are installed first because they are associated with a lower cost coefficient compared to that of units 1 and 2. Also, following more than 60% increase in the load, the microgrid planning solution would install candidate lines, as represented in Table 4.6, which causes a sudden increase in the investment cost. On the other hand, by increasing the total load, more power is generated by DGs, and more power would be imported from the utility grid, which cause the operation cost, and hence the planning cost, to increase.

Table 4.6 Investment Plan with Respect to Load Changes

Load Change Coefficient	1	2	3	4	5	6	Installed Lines
Original Load	0	0	0.10	1.00	0	0.48	-
+20%	0	0	0.31	1.00	0	0.52	
+40%	0	0	0.53	1.00	0	0.55	-
+60%	0	0	0.75	1.00	0	0.58	38
+80%	0.02	0.14	0.80	1.00	0	0.91	33,34,36,38,40,41,42
+100%	0.03	0.31	0.84	1.00	0.10	0.96	33,34,35,36, 37,38,39,40,42

Table 4.7 Microgrid Costs with Respect to Load Changes

Load Change Coefficient	Investment Cost ($)	Operation Cost ($)	Planning Cost ($)
Original Load	1,310,805	8,151,773	9,462,578
+20%	1,497,853	9,961,260	11,459,113
+40%	1,683,933	11,734,030	13,417,963
+60%	1,876,168	13,594,840	15,471,008
+80%	2,644,088	14,884,100	17,528,188
+100%	2,904,977	16,729,010	19,633,987

Case 3: In this case, market prices are changed from -80% to +80%, and their impact on planning results is studied. Price changes are studied in two cases of considering and ignoring line installations. The planning results are represented in Tables 4.8 and 4.9. By 20% decrease in the market price, the total dispatchable capacity would remain unchanged, but unit 1 is also installed as its capital cost is relatively low, and as the market price has decreased. Therefore, it is financially beneficial to dispatch unit 1 instead of increasing the installed capacity of units 3 and 4. By 40% decrease in market prices, units 3 and 4 are not installed anymore, but unit 1 is installed with a higher capacity, as its annualized investment cost is lower. By additional reduction in the market price up to -80%, the solar unit is not installed either, and only a capacity of 1.09 MW of unit 1 is installed. This is due to the very low market price which makes it more economical to buy power from the utility grid. Unit 1 is installed in this case for the mere purpose of supplying critical loads. On the other hand, by increasing the market price, it would be desirable for the microgrid to generate more power in order to sell back to the utility grid (associated with negative exchange power with the utility grid in many hours), which causes the operation cost to drop. Therefore, more DG capacity would be installed. For more than 40% increase in the market price, a number of

distribution lines become congested, therefore, candidate lines are also installed, which would cause an increase in the investment cost. By increasing the market price, the decrease in the operation cost would be more dominant over the increase in the investment cost, so the planning cost would increase and then decrease. As shown in Table 4.9, for the values of percentage change in market prices that candidate lines are installed, the planning cost is lower than the case without allowing the installation of candidate lines. It means that the simultaneous installation of DGs and candidate lines would be economically more viable than installation of only DGs. Also, it should be mentioned that the DES is not installed for any change in market prices.

Table 4.8 Investment Plan with Respect to Market Price Changes

Price Change Coefficient		1	2	3	4	5	6	Installed Lines
-80%	w/o lines	1.09	0	0	0	0	0	-
	w/ lines	1.09	0	0	0	0	0	-
-60%	w/o lines	1.09	0	0	0	0	0	-
	w/ lines	1.09	0	0	0	0	0	-
-40%	w/o lines	1.09	0	0	0	0	0.48	-
	w/ lines	1.09	0	0	0	0	0.48	-
-20%	w/o lines	0.45	0	0	0.64	0	0.48	-
	w/ lines	0.45	0	0	0.64	0	0.48	-
Original Price	w/o lines	0	0	0.10	1.00	0	0.48	-
	w/ lines	0	0	0.10	1.00	0	0.48	-
+20%	w/o lines	0.32	0	0.67	1.00	0.12	0.48	-
	w/ lines	0.32	0	0.67	1.00	0.12	0.48	-
+40%	w/o lines	0.46	0	0.68	1.00	0.12	0.48	-
	w/ lines	0.75	0	0.68	1.00	0.21	0.77	34,35,36, 39,41
+60%	w/o lines	0.50	0	0.68	1.0	0.12	0.47	-
	w/ lines	0.79	0	0.68	1.0	0.21	0.77	34,35,39,41
+80%	w/o lines	0.62	0	0.68	1.0	0.19	0.44	-
	w/ lines	0.88	0	0.68	1.0	0.30	0.73	34,35,39,43

Table 4.9 Microgrid Costs with Respect to Market Price Changes

Price Change Coefficient		Investment Cost ($)	Operation Cost ($)	Planning Cost ($)
-80%	w/o lines	510,117	1,957,936	2,468,053
	w/ lines			
-60%	w/o lines	510,117	3,915,872	4,425,989
	w/ lines			
-40%	w/o lines	1,106,618	5,270,609	6,377,227
	w/ lines			
-20%	w/o lines	1,225,734	6,883,798	8,109,532
	w/ lines			
Original Price	w/o lines	1,310,805	8,151,773	9,462,578
	w/ lines			
+20%	w/o lines	1,988,144	8,298,427	10,286,571
	w/ lines			
+40%	w/o lines	2,059,625	8,622,853	10,682,478
	w/ lines	2,824,677	7,354,827	10,179,504
+60%	w/o lines	2,078,623	8,893,008	10,971,631
	w/ lines	2,831,566	7,307,358	10,138,924
+80%	w/o lines	2,174,184	9,012,843	11,187,027
	w/ lines	2,883,257	7,110,567	9,993,824

4.4.2 Preprocessing Approach to Identify Uncertainties

A microgrid is installed for a group of electricity customers with a peak load demand of 17 MW. The set of DERs used in this study is the same as what was considered in Section 2.3. The cost coefficients of dispatchable units 1-4 are considered to be $27.7/MWh, $39.1/MWh, $61.3/MWh, and $65.6/MWh, respectively. The upper and lower bounds for all sources of uncertainty are considered to be 10% of the forecasted data. The microgrid optimal scheduling problem is implemented on a high performance computing server consisting of four 10-core Intel Xeon E7-4870 2.4 GHz processors with 128 GB memory. The problem was formulated by MIP (for the robust

optimization problem) and linear programming (for the primal problem in the proposed approach) and solved by CPLEX 12.6 [56]. Two cases are studied to validate the accuracy of the proposed approach as well as its impact on reducing the computational complexity.

Case 1 (Validation): The proposed preprocess approach in uncertainty consideration is applied to the test microgrid to ensure its viability in identifying uncertainties for loads, renewable generation, and market prices. By increasing the budget of uncertainty option in the load from 0 to 24 and solving the dual problem, the order of hours that cause the worst-cases would be 17, 18, 19, 20, 16, 21, 14, 15, 22, 13, 12, 23, 24, 11, 10, 8, 9, 6, 7, 5, 4, 1, 3, and 2. The calculations of the proposed signal for load uncertainties, i.e., $\lambda_b(\widetilde{PD}_b + \overline{PD}_b)$, are shown in Fig. 4.2. By sorting the calculated values in all hours, it can be seen that the results would be the same as those obtained by solving the dual problem, meaning that the term $\lambda_b(\widetilde{PD}_b + \overline{PD}_b)$ would be a proper signal to assess the load uncertainty. Similarly, for the renewable generation, by increasing the budget of uncertainty option in renewable generation units from 0 to 24 and solving the dual problem, the order of hours that cause the worst-case realization with respect to the wind generation would be 21, 22, 13, 12, 14, 11, 6, 8, 9, 5, 7, 10, 17, and 18. Similarly, the order of hours that cause the worst-case realization with respect to the solar generation would be 17, 16, 18, 20, 15, 14, 19, 13, and 12. The wind and solar generation in other hours is zero. The calculations of the proposed signal for wind and solar uncertainties, i.e., $\vartheta_{ib}(\tilde{P}_{ib} - \underline{P}_{ib})$, are shown in Fig. 4.3. By sorting the calculated values in all hours, it can be seen that the results would be the same as those

obtained by solving the dual problem, meaning that the term $\vartheta_{it}(\tilde{P}_{it} - \underline{P}_{it})$ would be a proper signal to assess the renewable generation uncertainty.

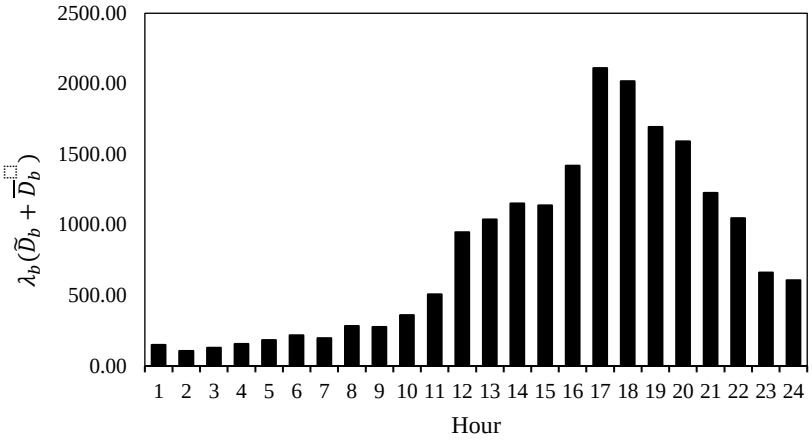

Fig. 4.2 Impact of the proposed signal for load uncertainties.

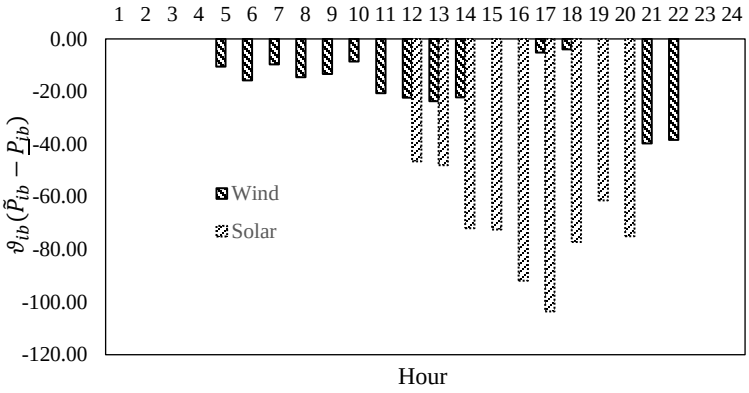

Fig. 4.3 Impact of the proposed signal for renewable uncertainties.

For the market price uncertainty, first it is assumed that there is not any storage unit. By increasing the budget of uncertainty option in market prices from 0 to 24 and solving the dual problem, the order of hours that cause the worst-case realization would be 12, 22, 21, 8, 9, 10, 6, 7, 16, 4, 5, 11, 1, 20, 17, 3, 19, 2, 18, 24, and 13. The calculated signal for market price uncertainties, i.e., $\Delta\rho_b . P_{M,b} + \Delta P_{ib} . (c_i - \rho_b - \Delta\rho_b)$, is shown in Fig. 4.4. It should be noted that 10% change in the market price would cause dispatchable unit 1 in hour 10, unit 2 in hour 11, unit 4 in hour 15, and unit 3 in hour 23

to be turned on. It also causes dispatchable unit 4 in hours 12 and 22 and also units 3 and 4 in hours 13 and 14 to be turned off. Therefore, as discussed in Section 4.3, the second term of the proposed signal, i.e., $\Delta P_{ib}.(c_i - \rho_b - \Delta\rho_b)$, should be considered for calculations at the aforementioned hours. By sorting the calculated values in all hours, it can be seen that the results would be the same as those obtained by solving the dual problem, meaning that $\Delta\rho_b.P_{M,b} + \Delta P_{ib}.(c_i - \rho_b - \Delta\rho_b)$ is a proper signal to assess the market price uncertainty. By considering DES in the assessment of market price uncertainties, the results calculated by the signal are slightly different from those obtained by solving the dual problem. However, the differences are marginal and can be ignored with acceptable accuracy.

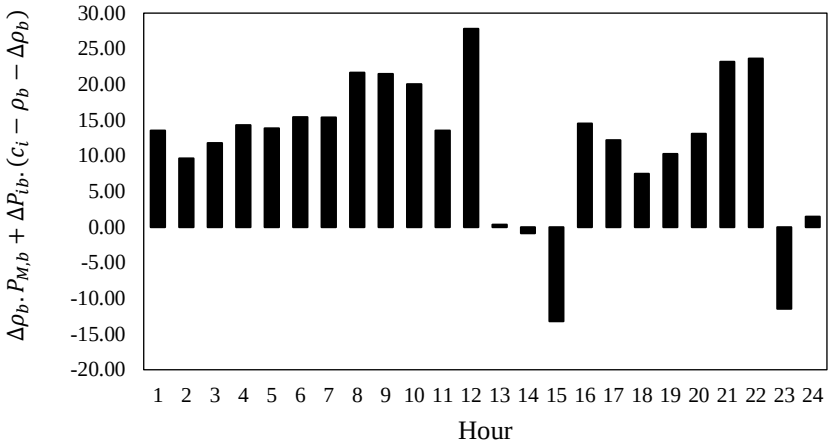

Fig. 4.4 Impact of the proposed signal for market price uncertainties.

Case 2 (Evaluation): The optimal scheduling problem is formulated using MIP and extended to obtain a one-year planning problem based on the data in [48]. There are eight sets of binary variables in the robust problem associated with upper and lower bounds of uncertainty intervals: two sets for the load, two sets for each of the two renewable generation units, and two sets for market prices. Each variable should be

defined at every single hour during the scheduling period, therefore there would be 70,080 (= 8×8760) binary variables which should be determined in order to find the worst-case realization. Such a large number of binary variables would considerably increase the computational complexity. The number of binary variables will also be further larger when: 1) a longer planning time horizon, e.g., 20 years, is considered, and 2) a shorter operation time period, e.g., 10-min operation to capture renewable generation variability instead of the hourly scheduling, is considered. In either case, the obtained robust problem will be significantly larger and noticeably more difficult to solve considering the large number of added binary variables.

The comparison between the two methods for a one-year planning problem is shown in Table 4.10. The proposed method in this work, which introduces signals to determine uncertainties, does not employ binary variables and formulates the problem using linear programming. The results show that reducing the number of variables and constraints would significantly decrease the computation time from 2.5-4 hours to less than a minute.

Table 4.10 Comparison Between the Robust Optimization Problem and the Proposed Preprocessing Approach

	Robust Optimization with Dual Variables	Proposed Uncertainty Preprocessing
Number of Continuous Variables	201,480	87,600
Number of Binary Variables	70,080	0
Number of Constraints	411,725	122,640
Computation Time	2.5-4 hours	~20 seconds

5. Chapter Five: Conclusion and Future Directions

Amongst different categories of microgrids, i.e., AC, DC and hybrid, extensive research has been conducted in the operation and control of AC microgrids. DC microgrids could however offer several advantages compared to AC microgrids: providing a more efficiently supply of DC loads and reducing losses due to the reduction of multiple converters used for DC loads, easier integration of DC DERs, and eliminating the need for synchronizing generators. In this dissertation, various components of AC, DC, and hybrid microgrids were explained, followed by developing a microgrid planning model. The model determined the optimal DER generation mix, size, and location, the optimal type of feeders in the microgrid, i.e., either AC or DC, as well as the threshold ratio of AC/DC loads at each feeder causing one type of feeder to be more economical than the other. In other words, for ratios smaller than the threshold ratio, AC microgrid would be more economical and for ratios larger than that, DC microgrid would be more economical. The problem objective was to minimize the total planning cost (comprising the investment cost of DERs and converters, the operation cost of dispatchable DGs and energy exchange with the utility grid, as well as the cost of unserved energy) subject to prevailing planning and operation constraints and was formulated using MILP. Numerical results were presented to analyze the impact of ratio of DC loads, ratio of critical loads, converters efficiency, and market price on microgrid planning solutions. It was verified that the decisive factor in determining the type of the

microgrid would be the ratio of DC loads. In other words, if other parameters change except for the ratio of DC loads, the type of the microgrid would not change. It was also shown that increasing the ratio of critical loads would increase the total installed dispatchable generation capacity. It was further demonstrated that changing critical loads, converters efficiency, or the market price, significantly affects the operation and reliability costs.

Moreover, a microgrid co-optimization generation and distribution planning was proposed in this dissertation, with the objective of determining the optimal DER generation mix and upgrading the network by building new lines. The nonlinear power flow equations were linearized to formulate the problem by MILP. The problem was tested on the IEEE 33-bus standard system, demonstrating the sensitivity of the planning results with respect to various planning factors, including the ratio of critical loads, total aggregated load, and electricity prices. Obtained results advocated that microgrid planners can ensure better planning economics by considering a simultaneous expansion in generation and distribution as opposed to traditional models focused only on generation expansion.

Furthermore, a detailed discussion and analysis of uncertainties in the microgrid optimal scheduling problem were provided in this dissertation. The least-cost operation objective was maximized over uncertainty sets, using robust optimization, to achieve the worst-case optimal solution in the microgrid day-ahead operation and accordingly capture forecast uncertainties. To address the computational complexity associated with the robust optimization model, a preprocess approach was proposed which was capable of identifying uncertainties without the need to formulate and solve the robust problem.

Instead, the preprocessing approach relied on solving the original linear problem and accordingly creating a set of uncertainty signals to identify the worst-case realizations of uncertain parameters. Based on the proposed preprocess approach, it was shown that the worst-case realization for load would occur at its upper bound, and for renewable generation at its lower bound. The worst-case realization for the market prices were contingent on whether the microgrid was selling power to or buying power from the utility grid. Numerical examples demonstrated that the proposed signals can accurately determine worst-case realization in load, renewable generation, and market prices, and the proposed approach was capable of significantly reducing the complexity and the computation time of microgrid operation and planning problems under uncertainty.

Considering that planning problems are big problems with a large number of binary and continuous variables over the planning horizon which is usually considered for 20-30 years, applying decomposition methods (such as Bender's Decomposition) could be considered as a future work. Bender's Decomposition converts the problem into a set of smaller and easier to solve, yet coordinated, subproblems. A suggested decomposition for the proposed microgrid planning problem would include a long-term investment master problem, a short-term operation subproblem, and a reliability subproblem. The investment plan obtained in the master problem will be examined in subproblems to find optimal DER schedule as well as desired levels of reliability. The final solution would be obtained in an iterative fashion.

References

[1] S. Parhizi, H. Lotfi, A. Khodaei, and S. Bahramirad, "State of the Art in Research on Microgrids: A Review," *IEEE Access*, vol. 3, pp. 890–925, 2015.

[2] M. Shahidehpour, "Role of smart microgrid in a perfect power system," in *IEEE PES General Meeting*, 2010, pp. 1–1.

[3] A. Flueck and Z. Li, "Destination: Perfection," *IEEE Power Energy Mag.*, vol. 6, no. 6, pp. 36–47, 2008.

[4] M. Shahidehpour and J. F. Clair, "A Functional Microgrid for Enhancing Reliability, Sustainability, and Energy Efficiency," *Electr. J.*, vol. 25, no. 8, pp. 21–28, Oct. 2012.

[5] S. Bahramirad, W. Reder, and A. Khodaei, "Reliability-Constrained Optimal Sizing of Energy Storage System in a Microgrid," *IEEE Trans. Smart Grid*, vol. 3, no. 4, pp. 2056–2062, Dec. 2012.

[6] A. G. Tsikalakis and N. D. Hatziargyriou, "Centralized control for optimizing microgrids operation," in *2011 IEEE Power and Energy Society General Meeting*, 2011, pp. 1–8.

[7] B. Kroposki, R. Lasseter, T. Ise, S. Morozumi, S. Papathanassiou, and N. Hatziargyriou, "Making microgrids work," *IEEE Power Energy Mag.*, vol. 6, no. 3, pp. 40–53, May 2008.

[8] A. Khodaei, "Microgrid Optimal Scheduling With Multi-Period Islanding Constraints," *IEEE Trans. Power Syst.*, vol. 29, no. 3, pp. 1383–1392, May 2014.

[9] S. Bahramirad, A. Khodaei, J. Svachula, and J. R. Aguero, "Building Resilient Integrated Grids: One neighborhood at a time.," *IEEE Electrif. Mag.*, vol. 3, no.

1, pp. 48–55, Mar. 2015.

[10] “Microgrid Workshop Report August 2011-Department of Energy.” [Online]. Available: https://energy.gov/oe/downloads/microgrid-workshop-report-august-2011. [Accessed: 08-May-2017].

[11] *Microgrid Deployment Tracker 2Q15: Commercial/Industrial, Community, Utility Distribution, Institutional/Campus, Military, Remote, and DC Microgrids: Operating, Planned, and Proposed Projects by World Region, May 2015.* .

[12] “Microgrid Deployment Tracker 4Q16.” [Online]. Available: https://www.navigantresearch.com/research/microgrid-deployment-tracker-4q16.

[13] Navigant Research, “Microgrid Deployment Tracker 2Q17,” 2017. [Online]. Available: https://www.navigantresearch.com/news-and-views/navigant-research-identifies-1842-microgrid-projects-representing-nearly-20-gw-of-capacity. [Accessed: 04-Apr-2019].

[14] “Microgrid Deployment Tracker 2Q18,” *Navigant Research*, 2018. [Online]. Available: https://www.navigantresearch.com/reports/microgrid-deployment-tracker-2q18. [Accessed: 24-Mar-2019].

[15] A. Forni, “Microgrid Deployment Tracker 4Q18,” *Navigant Research*, 2018. [Online]. Available: https://www.navigantresearch.com/reports/microgrid-deployment-tracker-4q18. [Accessed: 19-Mar-2019].

[16] P. Cairoli and R. A. Dougal, “New Horizons in DC Shipboard Power Systems: New fault protection strategies are essential to the adoption of dc power

systems.," *IEEE Electrif. Mag.*, vol. 1, no. 2, pp. 38–45, Dec. 2013.

[17] A. Khodaei, S. Bahramirad, and M. Shahidehpour, "Microgrid Planning Under Uncertainty," *IEEE Trans. Power Syst.*, vol. 30, no. 5, pp. 2417–2425, Sep. 2015.

[18] Ching-Chih Huang, Min-Jui Chen, Yung-Tang Liao, and Chan-Nan Lu, "DC microgrid operation planning," in *2012 International Conference on Renewable Energy Research and Applications (ICRERA)*, 2012, pp. 1–7.

[19] Q. Zhou, M. Shahidehpour, Z. Li, and X. Xu, "Two-Layer Control Scheme for Maintaining the Frequency and the Optimal Economic Operation of Hybrid AC/DC Microgrids," *IEEE Trans. Power Syst.*, vol. 34, no. 1, pp. 64–75, Jan. 2019.

[20] Y. Gu *et al.*, "Transfverter: imbuing transformer-like properties in an interlink converter for robust control of a hybrid ac-dc microgrid," *IEEE Trans. Power Electron.*, pp. 1–1, 2019.

[21] M. Baranwal, A. Askarian, S. Salapaka, and M. Salapaka, "A Distributed Architecture for Robust and Optimal Control of DC Microgrids," *IEEE Trans. Ind. Electron.*, vol. 66, no. 4, pp. 3082–3092, Apr. 2019.

[22] B. Papari, C. S. Edrington, and D. Gonsoulin, "Optimal energy-emission management in hybrid AC-DC microgrids with vehicle-2-grid technology," *J. Renew. Sustain. Energy*, vol. 11, no. 1, p. 015902, Jan. 2019.

[23] A. R. Yasin, M. Ashraf, A. I. Bhatti, and A. A. Uppal, "Fixed frequency sliding mode control of renewable energy resources in DC micro grid," *Asian J. Control*, Mar. 2019.

[24] F. Ornelas-Tellez, J. J. Rico-Melgoza, E. Espinosa-Juarez, and E. N. Sanchez,

"Optimal and Robust Control in DC Microgrids," *IEEE Trans. Smart Grid*, vol. 9, no. 6, pp. 5543–5553, Nov. 2018.

[25] X. Lu, N. Liu, Q. Chen, and J. Zhang, "Multi-objective optimal scheduling of a DC micro-grid consisted of PV system and EV charging station," in *2014 IEEE Innovative Smart Grid Technologies - Asia (ISGT ASIA)*, 2014, pp. 487–491.

[26] V. K. Hema and R. Dhanalakshmi, "Analysis of power sharing on hybrid AC-DC microgrid," in *2014 Annual International Conference on Emerging Research Areas: Magnetics, Machines and Drives (AICERA/iCMMD)*, 2014, pp. 1–6.

[27] N. Eghtedarpour and E. Farjah, "Power Control and Management in a Hybrid AC/DC Microgrid," *IEEE Trans. Smart Grid*, vol. 5, no. 3, pp. 1494–1505, May 2014.

[28] E. Shimoda, S. Numata, J. Baba, T. Nitta, and E. Masada, "Operation planning and load prediction for microgrid using thermal demand estimation," in *2012 IEEE Power and Energy Society General Meeting*, 2012, pp. 1–7.

[29] H. Kanchev, D. Lu, F. Colas, V. Lazarov, and B. Francois, "Energy Management and Operational Planning of a Microgrid With a PV-Based Active Generator for Smart Grid Applications," *IEEE Trans. Ind. Electron.*, vol. 58, no. 10, pp. 4583–4592, Oct. 2011.

[30] Z. Wu, P. Liu, W. Gu, H. Huang, and J. Han, "A bi-level planning approach for hybrid AC-DC distribution system considering N-1 security criterion," *Appl. Energy*, vol. 230, pp. 417–428, Nov. 2018.

[31] H. Pan *et al.*, "Research on Distributed Power Capacity and Site Optimization Planning of AC/DC Hybrid Micrograms Considering Line Factors," *Energies*,

vol. 11, no. 8, p. 1930, Jul. 2018.

[32] L. Zhang, Y. Chen, C. Shen, W. Tang, J. Liang, and B. Xu, “Optimal configuration of hybrid AC/DC urban distribution networks for high penetration renewable energy,” *IET Gener. Transm. Distrib.*, vol. 12, no. 20, pp. 4499–4506, Nov. 2018.

[33] O. Hafez and K. Bhattacharya, “Optimal planning and design of a renewable energy based supply system for microgrids,” *Renew. Energy*, vol. 45, pp. 7–15, Sep. 2012.

[34] E. Planas, J. Andreu, J. I. Gárate, I. Martínez de Alegría, and E. Ibarra, “AC and DC technology in microgrids: A review,” *Renew. Sustain. Energy Rev.*, vol. 43, pp. 726–749, Mar. 2015.

[35] E. Unamuno and J. A. Barrena, “Hybrid ac/dc microgrids—Part II: Review and classification of control strategies,” *Renew. Sustain. Energy Rev.*, vol. 52, pp. 1123–1134, Dec. 2015.

[36] I. Prodan, E. Zio, and F. Stoican, “Fault tolerant predictive control design for reliable microgrid energy management under uncertainties,” *Energy*, vol. 91, pp. 20–34, 2015.

[37] A. Zidan, H. A. Gabbar, and A. Eldessouky, “Optimal planning of combined heat and power systems within microgrids,” *Energy*, vol. 93, pp. 235–244, 2015.

[38] A. Karabiber, C. Keles, A. Kaygusuz, and B. B. Alagoz, “An approach for the integration of renewable distributed generation in hybrid DC/AC microgrids,” *Renew. Energy*, vol. 52, pp. 251–259, 2013.

[39] F. Nejabatkhah and Y. W. Li, “Overview of Power Management Strategies of

Hybrid AC/DC Microgrid," *IEEE Trans. Power Electron.*, vol. 30, no. 12, pp. 7072–7089, Dec. 2015.

[40] M. Zachar and P. Daoutidis, "Understanding and predicting the impact of location and load on microgrid design," *Energy*, vol. 90, pp. 1005–1023, 2015.

[41] V. Salehi, A. Mohamed, and O. A. Mohammed, "Implementation of real-time optimal power flow management system on hybrid AC/DC smart microgrid," in *2012 IEEE Industry Applications Society Annual Meeting*, 2012, pp. 1–8.

[42] N. N. Mansor, "Distribution planning considering network contingencies and switchgear relocation," in *2016 IEEE PES Innovative Smart Grid Technologies Conference Europe (ISGT-Europe)*, 2016, pp. 1–6.

[43] B. Nasiri, C. Wagner, A. Ahsan, and U. Hager, "A new perspective for smart distribution grid planning," in *2016 IEEE International Conference on Power System Technology (POWERCON)*, 2016, pp. 1–6.

[44] S. Sarabi, A. Davigny, V. Courtecuisse, L. Coutard, and B. Robyns, "Distribution grid planning enhancement using profiling estimation technic," in *CIRED Workshop 2016*, 2016, p. 82 (4 .)-82 (4 .).

[45] S. Karagiannopoulos, P. Aristidou, A. Ulbig, S. Koch, and G. Hug, "Optimal planning of distribution grids considering active power curtailment and reactive power control," in *2016 IEEE Power and Energy Society General Meeting (PESGM)*, 2016, pp. 1–5.

[46] J. Dominguez, J. P. Chaves-Avila, T. G. S. Roman, and C. Mateo, "The economic impact of demand response on distribution network planning," in *2016 Power Systems Computation Conference (PSCC)*, 2016, pp. 1–7.

[47] A. Khodaei and M. Shahidehpour, "Microgrid-Based Co-Optimization of Generation and Transmission Planning in Power Systems," *IEEE Trans. Power Syst.*, vol. 28, no. 2, pp. 1582–1590, May 2013.

[48] H. Lotfi and A. Khodaei, "AC Versus DC Microgrid Planning," *IEEE Trans. Smart Grid*, vol. 8, no. 1, pp. 296–304, Jan. 2017.

[49] J. Frayer, S. Keane, and J. Ng, "Estimating the Value of Lost Load," 2013. [Online]. Available: http://www.ercot.com/content/gridinfo/resource/2015/mktanalysis/ERCOT_ValueofLostLoad_LiteratureReviewandMacroeconomic.pdf. [Accessed: 07-May-2017].

[50] C.-K. Woo and R. L. Pupp, "Costs of service disruptions to electricity consumers," *Energy*, vol. 17, no. 2, pp. 109–126, Feb. 1992.

[51] Y. L. Mok, "Prediction of domestic, industrial and commercial interruption costs by relational approach," in *APSCOM-97. International Conference on Advances in Power System Control, Operation and Management*, 1997, vol. 1997, pp. 209–215.

[52] "Microgrid at Illinois Institute of Technology." [Online]. Available: http://www.iitmicrogrid.net/microgrid.aspx. [Accessed: 08-May-2017].

[53] S. Schoenung, "Energy Storage Systems Cost Update," 2011. [Online]. Available: http://prod.sandia.gov/techlib/access-control.cgi/2011/112730.pdf. [Accessed: 08-May-2017].

[54] "NREL: Distributed Generation Renewable Energy Estimate of Costs." [Online]. Available: http://www.nrel.gov/analysis/tech_lcoe_re_cost_est.html. [Accessed:

08-May-2017].

[55] R. Remick and D. Wheeler, “Molten Carbonate and Phosphoric Acid Stationary Fuel Cells: Overview and Gap Analysis,” 2010. [Online]. Available: https://www1.eere.energy.gov/hydrogenandfuelcells/pdfs/49072.pdf. [Accessed: 08-May-2017].

[56] “IBM ILOG CPLEX Optimization Studio V12.6.3 documentation.” [Online]. Available: https://www.ibm.com/support/knowledgecenter/SSSA5P_12.6.3/ilog.odms.studio.help/Optimization_Studio/topics/COS_home.html. [Accessed: 07-May-2017].

[57] H. Lotfi and A. Khodaei, “Hybrid AC/DC microgrid planning,” *Energy*, vol. 118, pp. 37–46, 2017.

[58] H. Lotfi and A. Khodaei, “An efficient preprocessing approach for uncertainty consideration in microgrids,” in *2016 IEEE/PES Transmission and Distribution Conference and Exposition (T&D)*, 2016, pp. 1–5.

[59] H. Lotfi and A. Khodaei, “AC Versus DC Microgrid Planning,” *IEEE Trans. Smart Grid*, vol. 8, no. 1, pp. 296–304, Jan. 2017.

[60] A. Alanazi, H. Lotfi, and A. Khodaei, “Coordinated AC/DC microgrid optimal scheduling,” in *2017 North American Power Symposium (NAPS)*, 2017, pp. 1–6.

[61] A. Gupte, S. Ahmed, M. S. Cheon, and S. Dey, “Solving Mixed Integer Bilinear Problems Using MILP Formulations,” *SIAM J. Optim.*, vol. 23, no. 2, pp. 721–744, Jan. 2013.

[62] W. Albeck and S. Estomin, “Cost Benefits for Overhead vs. Underground

Utilities."

[63] H. Lotfi and A. Khodaei, "Static hybrid AC/DC microgrid planning," in *2016 IEEE Power & Energy Society Innovative Smart Grid Technologies Conference (ISGT)*, 2016, pp. 1–5.